# Distribution of White Matter Hyperintensities across Arterial Territories in Neurodegenerative Diseases

Ikrame Housni[1,2,3,4], Flavie E. Detcheverry[1,2,3,4], Manpreet Singh[1,2,3,4], Mahsa Dadar[5,6], Chloe Anastassiadis[7], Ali Filali-Mouhim[3], Mario Masellis[8], Zahinoor Ismail[9,10], Eric E. Smith[10], Simon Duchesne[11, 12], Maria Carmela Tartaglia[7,13], Natalie A. Phillips[14], Sridar Narayanan[15,16], AmanPreet Badhwar[1,2,3,4 *]

[1]Multiomics investigation of neurodegenerative diseases (MIND) Laboratory, Montréal, Canada; [2]Département de pharmacologie et physiologie, Faculté de médecine, Université de Montréal, Montreal, QC, Canada; [3]Centre de Recherche de l'Institut Universitaire de Gériatrie de Montréal (CRIUGM), Montreal, QC, Canada; [4]Institut de génie biomédical, Université de Montréal, Montreal, QC, Canada; [5]Department of Psychiatry, McGill University, Montreal, QC, Canada; [6]Douglas Mental Health University Institute, Montreal, QC, Canada; [7]Tanz Centre for Research in Neurodegenerative Diseases, Toronto, ON, Canada; [8]Division of Neurology, Department of Medicine, Sunnybrook Health Sciences Centre, University of Toronto & Cognitive Neurology Research Unit, Hurvitz Brain Sciences Program, Sunnybrook Research Institute, Toronto, ON, Canada; [9]Department of Psychiatry, Hotchkiss Brain Institute, University of Calgary, Calgary, AB, Canada; [10]Department of Clinical Neurosciences and Hotchkiss Brain Institute, University of Calgary, Calgary, AB, Canada; [11]Département de radiologie et médecine nucléaire, Université Laval, Quebec, QC, Canada; [12]Quebec Heart and Lung Institute, QC, Canada; [13]Krembil Brain Institute, University Health Network, Toronto, ON, Canada; [14]Department of Psychology, Concordia University; [15]McConnell Brain Imaging Centre, Montreal Neurological Institute, Montreal, QC, Canada; [16]Department of Neurology and Neurosurgery, McGill University, Montreal, QC, Canada.

* Corresponding author: AmanPreet Badhwar, MSc, PhD

[2]Multiomics Investigation of Neurodegenerative Diseases (MIND) lab, 4545 Chemin Queen May, Montréal, QC, H3W 1W4, Canada; [3]Centre de Recherche de l'Institut Universitaire de Gériatrie de Montréal (CRIUGM), 4545 Chemin Queen May, Montréal, QC, H3W 1W4, Canada; [4]Department of Pharmacology and Physiology, Université de Montréal, 2900 Boulevard Édouard-Montpetit, Montréal, QC, H3T 1J4, Canada; [5]Institute of Biomedical Engineering, Université de Montréal, 2960 Chemin de la Tour, Montréal, QC, H3T 1J4, Canada.

E-mail: amanpreet.badhwar@umontreal.ca

Fax number: 001 (514) 340-3530

Work phone: 001 (514) 340-3540, extension 3345

Postal address: 4565, chemin Queen Mary, Montreal, QC, Canada, H3W 1W5

## ABSTRACT

MRI-detected white matter hyperintensities (WMH) are often recognized as markers of cerebrovascular abnormalities and an index of vascular brain injury. The literature establishes a strong link between WMH burden and cognitive decline, and suggests that the anatomical distribution of WMH mediates cognitive dysfunction. Pathological remodeling of major cerebral arteries (anterior, ACA; middle, MCA; posterior, PCA) may increase WMH burden in an arterial territory (AT)-specific manner. However, this has not been systematically studied across neurodegenerative diseases (NDDs). To address this gap, we aimed to assess WMH distribution (i) across ATs per clinical category, (ii) across clinical categories per AT, and (iii) between men and women. We also investigated the association between AT-specific WMH burden and cognition.

Using two cohorts – Canadian CCNA-COMPASS-ND (N=927) and US-based NIFD (N=194) – we examined WMH distribution across ten clinical categories: cognitively unimpaired (CU), subjective cognitive decline (SCD), mild cognitive impairment (MCI), Alzheimer disease (AD), MCI and AD with high vascular injury (+V), Lewy body dementia, frontotemporal dementia, Parkinson's disease (PD), and PD with cognitive impairment or dementia. WMH masks were segmented from FLAIR MRI and mapped onto an arterial atlas. Cognitive performance was assessed using four psychometric tests evaluating reaction time and overall cognition, namely Simple Reaction Time (SRT), Choice Reaction Time (CRT), Digit Symbol Substitution Test (DSST), and Montreal Cognitive Assessment (MoCA). Statistical analyses involved linear regression models, controlling for demographic factors, with a 5% False Discovery Rate for multiple comparisons.

Our transdiagnostic analysis revealed unique AT-specific WMH burden patterns. Comparisons between ACA and PCA territories revealed distinct burden patterns in clinical categories with similar whole-brain WMH burden, while the MCA territory consistently exhibited the highest burden across all categories, despite accounting for AT size. Hemispheric asymmetries were noted in seven diagnostic categories, with most showing higher WMH burden in the left MCA territory. Our results further revealed distinct AT-specific WMH patterns in diagnostic groups that are more vascular than neurodegenerative (i.e., MCI+V, AD+V). Categories often misdiagnosed in clinical practice, such as FTD and AD, displayed contrasting WMH signatures across ATs. SCD showed distinct AT-specific WMH patterns compared to CU and NDD participants. Additionally,

sex-specific differences emerged in five NDDs, with varying AT effects. Importantly, AT-specific WMH burden was associated with slower processing speed in MCI (PCA) and AD (ACA, MCA).

This study highlights the importance of evaluating WMH distribution through a vascular-based brain parcellation. We identified ATs with increased vulnerability to WMH accumulation across NDDs, revealing distinct WMH signatures for multiple clinical categories. In the AD continuum, these signatures correlated with cognitive impairment, underscoring the potential for vascular considerations in imaging criteria to improve diagnostic precision.

**KEYWORDS**

White matter hyperintensities (WMH); Neurodegenerative diseases (NDDs); Arterial territories (ATs); Cerebrovasculature; Imaging biomarkers

## 1. INTRODUCTION

The world population is aging, and the rise of age-related neurodegenerative diseases (NDDs) poses a major health challenge [1–3], with over 55 million people affected [4,5]. Of the NDDs, Alzheimer's disease (AD) is the most prevalent [6,7]. Mounting evidence indicates a pivotal role of cerebrovascular pathology in the initiation, progression, and/or exacerbation of NDDs [8–11]. Cerebrovascular pathology features routinely detected by non-invasive *in vivo* magnetic resonance imaging (MRI) are white matter hyperintensities (WMH), covert brain infarcts, microbleeds, lacunes, and enlarged perivascular spaces, with WMH being the most common [12,13]. A recent meta-analysis investigating these four features found only WMH burden to be significantly associated with increased risk of dementia (including AD) in the general population [12].

WMH appear as areas of elevated signal in white matter on T2-weighted, proton density-weighted, or fluid-attenuated inversion recovery MRI [14]. Increased water content in brain white matter due to axonal damage (demyelination, loss), and to some extent edema, are thought to contribute to the appearance of WMH [15,16]. Putative vascular pathogenic mechanisms of WMH include endothelial and associated blood-brain-barrier dysfunction, hypoperfusion due to altered cerebrovascular autoregulation and reactivity, and cerebral amyloid angiopathy [16–25].

Emerging literature points to NDD-specific spatial distribution of WMH in the brain [26]. Examples include a significantly higher WMH burden in the (i) deep [27] and right-posterior [28] brain regions in vascular dementia compared to AD, and (ii) periventricular and subcortical regions in AD compared to Parkinson's disease (PD) [29]. Studies further suggest that these NDD-specific spatial distributions of WMH can impact cognitive function [11,26,29,30]. To date, the main analytical approaches utilized to map NDD-specific WMH topography consist of: region of interest (ROI)-based approaches, with most studies investigating WMH distribution in cortical lobes (e.g., frontal versus parietal); ventricular-based approaches, with studies assessing WMH distribution based on distance from ventricular surface (e.g., periventricular versus deep); and voxel-based approaches, with studies assessing presence of WMH in each white matter voxel [26]. Lacking, however, is an appreciation of the relationship of WMH location with respect to a cerebrovascular architecture (e.g., arterial-territory, -density) informed mapping.

Indeed, accumulating observations collectively point to a crucial need for cerebral arterial-territory (AT) informed mapping of NDD-specific distributions of WMH. Most of the brain, namely the supratentorial brain, is largely served by blood vessels arising from three major cerebral arteries (anterior, ACA; middle, MCA; posterior, PCA), properties of which can give rise to region-specific effects. For instance, lumen diameter and wall thickness of these arteries have been shown to correlate positively with lumen diameter of downstream ipsilateral arterioles [31]. Physiological (e.g., aging) or pathological remodeling of these arteries, therefore, has the potential to stimulate AT-specific remodeling of distal arterioles [31] and increase WMH burden [32]. In fact, cerebral arteries comprising the anterior (including ACA and MCA [33,34]) and posterior (including PCA [33,34]) circulation [35] differ in the distribution of age-specific histopathological features (e.g., elastin loss, increased collagen and/or amyloid-beta (Aβ) deposition), with dissimilarity in arterial properties of the two circulations (e.g., sympathetic innervation) as a contributing factor [36,37]. Moreover, emerging studies demonstrate that the spatial patterning of age-specific cerebrovascular pathology may modulate NDD-specific risk-factors and/or changes (e.g., *APOE-E4* allele, increased Aβ deposition) [38–42]. For example, age-related increase in collagen content in posterior relative to anterior circulation promotes Aβ accumulation, which may contribute to increased cerebral amyloid angiopathy in the posterior circulation [35,40] and the posterior predominance of WMH in AD [43].

To date, while AT-informed mapping of WMH distribution is lacking for NDDs, two non-NDD studies highlight the utility of conducting such investigations. The first study found that in cognitively unimpaired (CU) older adults (60-64 years of age), subregions of the ACA and MCA territories, supplied by the medial and lateral lenticulostriate arteries, respectively, exhibited the highest prevalence of WMH [44]. The second study investigated stroke, itself a risk factor for NDD [45] found that ACA WMH burden was most associated with stroke risk-factors over MCA and PCA [46].

In the present study, we conducted **AT-informed mapping of NDD-specific WMH distributions**, and hypothesized the presence of NDD-specific signatures. Our three main aims were to assess WMH volume (i) across ATs within each clinical category (Aim 1), (ii) across clinical categories per AT (Aim 2), and (iii) between men and women per clinical category and AT, given that sex-specific differences in WMH volume have been reported

[47] (Aim 3). Given that both increased WMH burden [48] and its anatomical distribution [11] mediate cognitive dysfunction, a follow-up aim (Aim 4) was to investigate the association between AT-specific WMH burden and cognition.

## 2. METHODS

### 2.1. Participants

***CCNA COMPASS-ND cohort***

We used participant data (demographic, cognition, cross-sectional MRI) from the Comprehensive Assessment of Neurodegeneration and Dementia (COMPASS-ND) cohort of the Canadian Consortium on Neurodegeneration in Aging (CCNA), a pan-Canadian initiative to catalyze and promote dementia-related research [49]. The 927 participants included were distributed across ten clinical categories, namely, CU (N=107), as well as subjective cognitive impairment or decline (SCD; N=133), mild cognitive impairment due to AD (MCI; N=240; i.e., the prodrome stage of AD), MCI with a high vascular brain injury (MCI+V; N=133), AD (N=93), AD with a high vascular brain injury (AD+V; N=46), Lewy body dementia (LBD; N=26), frontotemporal dementia (FTD; N=23), PD (N=77), and PD with cognitive impairment or dementia (PDD; N=49). Per participant, clinical diagnosis was determined by physicians based on standard diagnostic criteria following evaluation of information from recruitment assessment, screening visit, longitudinal clinical visits, and MRI [49]. Ethical agreements and written informed consents were obtained from all participants [49,50]. Information on availability and access to CCNA COMPASS-ND data can be requested at https://ccna-ccnv.ca/contact/.

***NIFD cohort***

Due to the low CCNA COMPASS-ND FTD sample size, we also included FTD participants from the Frontotemporal Lobar Degeneration Neuroimaging Initiative (FTLDNI also known as NIFD) to validate the replicability of our findings. The NIFD is a multi-site study funded through the National Institute of Aging that aims to identify neuroimaging biomarkers of FTD. In addition to our CCNA COMPASS-ND analyses, we conducted separate analyses on the sample collected at the primary collection site, which consisted of 194 participants distributed across two clinical categories, namely, cognitively unimpaired (CU_NIFD; N=96) and frontotemporal dementia (FTD_NIFD; N=98). Access to the dataset can be requested

from Laboratory of Neuro Imaging (LONI) (https://ida.loni.usc.edu/login.jsp) and further information can be found at https://4rtni-ftldni.ini.usc.edu/.

***Naming convention used for the CCNA COMPASS-ND and NIFD cohorts***

Our data included two FTD and CU groups from the CCNA COMPASS-ND and NIFD datasets. We use the terms "FTD" and "CU" specifically for groups from the CCNA COMPASS-ND cohort. For groups from the NIFD cohort, we use the terms "FTD_NIFD" and "CU_NIFD." This naming convention ensures clear differentiation between the cohorts throughout our analysis.

### 2.2. Magnetic Resonance Imaging Data

***CCNA COMPASS-ND cohort***

All CCNA COMPASS-ND participants were scanned following the Canadian Dementia Imaging Protocol (CDIP; [51]), a harmonized MRI protocol designed to reduce inter-scanner variability in multi-centre studies. MRI was performed using three 3 tesla (T) scanner models, namely GE, Philips, and Siemens. MRI sequences used to detect WMH included 3D isotropic T1-weighted and 2D T2-weighted fluid attenuated inversion recovery (slice thickness 3mm, FLAIR: TR 9000 ms, TI 2500) acquisitions.

***NIFD cohort***

3D T2-weighted FLAIR scans (slice thickness 1mm, TR 6000 ms, TE 389 ms, inversion time 2100 ms) and MPRAGE T1-weighted scans (slice thickness 1mm, TR 2300 ms, TE 3ms, TI 900 ms) were obtained on a 3T Siemens TrioTrim scanner for all participants, following a harmonized protocol based on Alzheimer's Disease Neuroimaging Initiative (ADNI) recommendations [52].

#### *2.2.1 MRI-preprocessing and WMH-segmentation*

***CCNA COMPASS-ND cohort***

MRI scans were downloaded from the CCNA COMPASS-ND LORIS database [53]. Image preprocessing, including (i) image denoising [54], (ii) correction for intensity non-uniformity [55], and (iii) normalization of image intensities (set range: 0-100), was performed as previously described [56]. FLAIR images were co-registered to the T1-weighted images using a 6-parameter rigid-body registration and mutual information cost function [56].

Images were visually assessed for artifacts to ensure successful registration before being included in our analyses.

WMH were segmented in native FLAIR space using a publicly available automated segmentation method [57–59]. All segmentations were visually quality controlled to ensure their accuracy. T1-weighted images were linearly registered (9 parameters) to the MNI-ICBM152-2009c template space using a cross-correlation objective function [56]. To adjust for brain size variations and enable atlas-based regional analyses, MRI images and WMH maps were linearly transformed to MNI standard space. WMH burden was assessed per ROI using an AT atlas [46] in standard space (Fig. 1).

***NIFD cohort***

WMH were segmented using the open-access Lesion Prediction Algorithm (LPA) from the Lesion Segmentation Toolbox (LST) [60] available for download at https://www.applied-statistics.de/lst.html, and run on SPM12 (Matlab 2020). The resulting lesion probability maps were thresholded at 0.4 and manual corrections were performed by C.A. (blinded to diagnosis) to improve segmentation quality in ITK-SNAP 3.8.0. [61] (http://www.itksnap.org/pmwiki/pmwiki.php?n=Main.HomePage). WMH maps were then spatially normalized to the ICBM152 linear template using SPM12. The WMH burden was assessed per ROI using an AT atlas [46] in standard space.

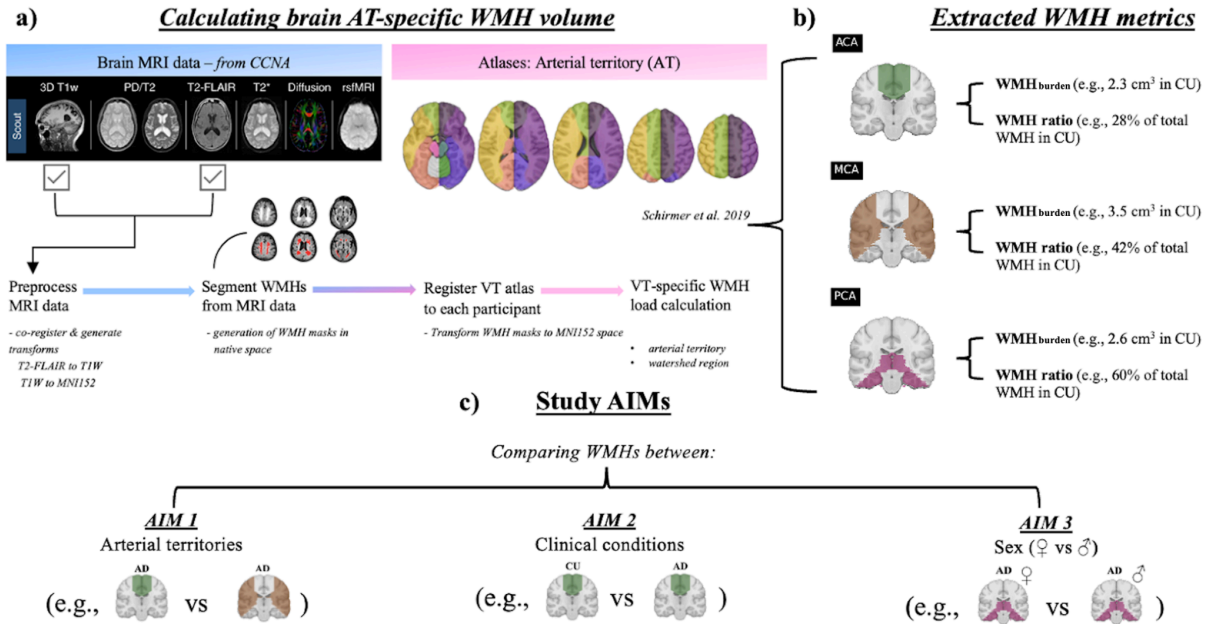

**Fig. 1. a-b)** Workflow for calculating AT-specific WMH metrics: regional *WMH burden*, *WMH ratio* (regional burden/whole-brain burden) – examples provided. **c)** Aims of completed study; *Aim 1*: comparing WMH burden across ATs, per clinical category, *Aim 2*: comparing AT-specific WMH metrics across clinical categories, *Aim 3*: comparing WMH metrics across sex per clinical category and AT.

### *2.2.2 Investigated ROIs*

We delineated ten ROIs from the supratentorial brain based on their vascular supply (Fig. 1a-b). Specifically, we concentrated our analysis on the major cerebral arteries, namely the ACA, MCA, and PCA. This macro-level approach allowed us to explore the three major networks of brain arteries. The analysis excluded the vertebro-basilar territory due to a significant decrease in data quality of FLAIR images in that region, rendering it insufficient for reliable use in our study. The included ROIs were grouped and statistically analyzed in three independent levels. **Level 1 (1 ROI):** *whole-brain* – supratentorial brain. **Level 2 (3 ROIs):** *bilateral ATs* – ACA territory ($ACA_t$), MCA territory ($MCA_t$), and PCA territory ($PCA_t$). **Level 3 (6 ROIs):** *lateral ATs* – left $ACA_t$ ($LACA_t$), $LMCA_t$, $LPCA_t$, and right $ACA_t$ ($RACA_t$), $RMCA_t$, $RPCA_t$. Statistical analyses were performed and adjusted for multiple comparisons within each level.

### *2.2.3 WMH metrics*

Two metrics were used to assess the spatial distribution of WMHs, per ROI, namely WMH burden and WMH ratio. The regional WMH burden represents the volume of WMH within a given ROI. AT-specific WMH burden was corrected for AT-size to control for differences in region size when comparing inter-AT WMH burden [46]. The WMH ratio represents the proportion of regional WMH burden relative to the overall WMH burden, per ROI. This was mathematically assessed by dividing a ROI's WMH burden by the whole-brain's WMH burden.

Note that whenever we examined WMH in the whole-brain (i.e., Aims 2 and 3), we only evaluated the WMH burden, as the WMH ratio (which controls for the WMH burden of the entire brain) would invariably yield a value of 1 whenever the whole-brain is the ROI. Similarly, in Aim 1, we exclusively compared AT-specific WMH burden, as comparing AT-specific WMH ratios within the same individual would involve fractions with identical denominators. Consequently, conducting WMH ratio analyses in addition to WMH burden analyses in Aim 1 would have been redundant.

## 2.3. Statistical Analysis

### *2.3.1 Analyses for AIMs 1-3: AT-specific WMH distributions*

All statistical analyses were performed using R statistical software (v 4.1.3; R Core Team 2022) [62]. A series of generalized linear models (GLMs) were used with log-transformed region-size normalized WMH load as the dependent variable and clinical category, age, and sex as independent variables followed by appropriate pairwise comparisons of the WMH metrics. After fitting the models, we tested the validity of the linear model by assessing the normality of the residuals on the fit. To perform these comparisons, the *emmeans* function in R (emmeans; v 4.1.3; R Core Team 2022) used our GLMs as input to calculate the Estimated Marginal Means (EMMs) of our factor levels (predicted mean response of each level), while adjusting for the effects of the other factors in the model [63]. Subsequently, pairwise comparisons were conducted between the EMMs of each level to determine the significant differences between our factor levels. A 5% False Discovery Rate (FDR) was used to correct for multiple comparisons, adjusted *p*-values are reported.

As the CCNA COMPASS-ND and NIFD cohorts used different acquisition and imaging protocols, we performed analyses separately within each dataset. This approach is taken to avoid measurement and selection biases due to acquisition differences, ensuring the comparisons are reliable. Therefore, for group pairwise comparisons, all ten CCNA COMPASS-ND diagnoses will be compared against each other within the CCNA COMPASS-ND cohort, while in the NIFD cohort, only FTD_NIFD and CU_NIFD will be compared.

***Inputted GLM models***

*Aim 1. WMH burden per clinical category ~ 1 +* ***ROIs*** *+ 1|Subject*

The model assessed differences in WMH burden between ROIs (variable of interest) for each clinical category, while ensuring subject pairing. Linear models and multiple comparison corrections were applied separately within CCNA COMPASS-ND and NIFD cohorts.

*Aim 2. WMH metric per ROI ~ 1 +* ***clinical category*** *+ Sex + Age*

The model assessed differences in regional WMH burden or ratio between clinical categories (variable of interest) for each ROI, while correcting for age and sex. Linear models and

multiple comparison corrections were applied separately within CCNA COMPASS-ND and NIFD cohorts.

*Aim 3. WMH metric per ROI and clinical category ~ 1 +* ***Sex*** *+ Age*

The model assessed differences in regional WMH burden or ratio between sexes (variable of interest) for each clinical category, while correcting for age. Linear models and multiple comparison corrections were applied within the CCNA COMPASS-ND cohort only.

### *2.3.2 Analyses for Aim 4: association between AT-specific WMH burden and cognition*

For Aim 4, we used cognitive assessments on a subset of our CCNA COMPASS-ND diagnostic groups, i.e., CU, SCD, MCI, AD, and MCI and AD with high vascular brain injury (N=756; Fig. 5a). Cognitive performance was operationalized as processing speed and cognitive screening using four psychometric tests: Simple Reaction Time (SRT), Choice Reaction Time (CRT), Digit Symbol Substitution Test (DSST), and Montreal Cognitive Assessment (MoCA) (Fig. 5b). SRT, CRT, and DSST evaluate processing speed, which is often one of the earliest cognitive functions to decline with age. The MoCA provides a broader screening of multiple cognitive domains, including executive function, memory, language, and visuospatial ability.

Statistical analyses involved a series of linear regression models, with cognitive performance as the dependent variable and region-size-normalized AT-WMH burden as the independent variable, adjusting for age and sex. A 5% False Discovery Rate threshold was applied to correct for multiple comparisons.

*Aim 4.1. Cognition ~ 1 +* ***WMH burden per ROI*** *+ Clinical category + Sex + Age*

Model assesses how the WMH burden (variable of interest) in specific brain regions is associated with cognitive performance (dependent variable), while adjusting for age, sex, and applying multiple comparison corrections. This analysis was conducted for each cognitive test and adjusting for diagnosis.

*Aim 4.2. Cognition ~ 1 +* ***WMH burden per ROI and clinical category*** *+ Sex + Age*

Model assesses how the WMH burden (variable of interest) in specific brain regions influences cognitive performance, while adjusting for age, sex, and applying multiple comparison corrections. This analysis was conducted for each cognitive test and diagnosis.

# 3. RESULTS

## 3.1 Cohort Demographics

### *CCNA COMPASS-ND cohort*

Brain-size normalized WMH burden values (in cubic centimeters, $cm^3$) per clinical category in each ROI are summarized in demographic Table 1.1 for the CCNA COMPASS-ND cohort. Participant ages ranged from 50 to 90 years old, with FTD being the youngest group and AD+V the oldest (Tables 1.1). Whole-brain WMH burden means ranged from 8.53±6.23 (CU) to 31.97±17.43 (AD+V) $cm^3$ in CCNA COMPASS-ND participants.

**Table 1.1** Demographic characteristics and WMH volumes (brain-size normalized and adjusted for AT-size values in cubic centimeters) for the CCNA COMPASS-ND participants used in this study, per clinical category. Participants from a total of ten clinical categories were included.

| | N | | | | WMH burden per region of interest (cm3) | | | | | | | | | |
|---|---|---|---|---|---|---|---|---|---|---|---|---|---|---|
| | Total | F | M | Age | Total | ACA | MCA | PCA | LACA | LMCA | LPCA | RACA | RMCA | RPCA |
| Diagnosis | | | | | M ± SD | M ± SD | M ± SD | M ± SD | M ± SD | M ± SD | M ± SD | M ± SD | M ± SD | M ± SD |
| CU | 107 | 81 | 26 | 70 ± 6.11 | 8.53 ± 6.23 | 0.82 ± 0.78 | 1.24 ± 0.96 | 0.93 ± 0.56 | 0.39 ± 0.39 | 0.67 ± 0.51 | 0.47 ± 0.30 | 0.43 ± 0.40 | 0.57 ± 0.46 | 0.46 ± 0.28 |
| SCD | 133 | 97 | 36 | 70.4 ± 5.98 | 10.79 ± 9.28 | 1.14 ± 1.37 | 1.62 ± 1.40 | 0.90 ± 0.49 | 0.53 ± 0.63 | 0.86 ± 0.74 | 0.43 ± 0.24 | 0.61 ± 0.76 | 0.76 ± 0.67 | 0.47 ± 0.29 |
| MCI | 240 | 99 | 141 | 72.1 ± 6.69 | 10.55 ± 8.20 | 1.05 ± 1.19 | 1.54 ± 1.25 | 1.10 ± 0.55 | 0.49 ± 0.58 | 0.81 ± 0.66 | 0.52 ± 0.27 | 0.56 ± 0.64 | 0.73 ± 0.61 | 0.58 ± 0.33 |
| MCI+V | 133 | 59 | 74 | 76.5 ± 6.3 | 29.94 ± 17.97 | 3.81 ± 3.07 | 4.45 ± 2.58 | 1.81 ± 0.90 | 1.77 ± 1.42 | 2.32 ± 1.33 | 0.85 ± 0.45 | 2.04 ± 1.69 | 2.12 ± 1.29 | 0.96 ± 0.51 |
| AD | 93 | 40 | 53 | 73.1 ± 7.79 | 14.02 ± 10.14 | 1.52 ± 1.83 | 1.98 ± 1.36 | 1.50 ± 0.73 | 0.73 ± 0.90 | 1.04 ± 0.73 | 0.71 ± 0.39 | 0.80 ± 0.96 | 0.94 ± 0.67 | 0.79 ± 0.40 |
| AD+V | 46 | 20 | 26 | 78.7 ± 5.59 | 31.97 ± 17.43 | 4.22 ± 3.20 | 4.60 ± 2.34 | 2.14 ± 0.93 | 2.05 ± 1.60 | 2.46 ± 1.23 | 1.10 ± 0.59 | 2.17 ± 1.65 | 2.14 ± 1.17 | 1.04 ± 0.44 |
| LBD | 26 | 4 | 22 | 73.3 ± 7.91 | 18.87 ± 14.15 | 2.20 ± 2.00 | 2.70 ± 2.07 | 1.70 ± 1.00 | 1.03 ± 0.92 | 1.39 ± 1.01 | 0.81 ± 0.44 | 1.17 ± 1.15 | 1.31 ± 1.09 | 0.89 ± 0.62 |
| FTD | 23 | 11 | 12 | 65.6 ± 8.89 | 17.39 ± 11.44 | 2.04 ± 1.84 | 2.49 ± 1.58 | 1.53 ± 0.81 | 0.92 ± 0.91 | 1.27 ± 0.86 | 0.82 ± 0.47 | 1.12 ± 0.96 | 1.22 ± 0.82 | 0.71 ± 0.40 |
| PD | 77 | 36 | 41 | 66.8 ± 7.2 | 9.91 ± 9.45 | 0.96 ± 1.12 | 1.51 ± 1.54 | 0.91 ± 0.57 | 0.47 ± 0.52 | 0.81 ± 0.83 | 0.44 ± 0.26 | 0.49 ± 0.61 | 0.70 ± 0.73 | 0.47 ± 0.36 |
| PDD | 49 | 7 | 42 | 72 ± 7.64 | 16.63 ± 12.80 | 1.76 ± 1.60 | 2.47 ± 2.03 | 1.49 ± 0.74 | 0.88 ± 0.88 | 1.34 ± 1.13 | 0.68 ± 0.37 | 0.88 ± 0.79 | 1.13 ± 0.93 | 0.81 ± 0.41 |

### *NIFD cohort*

Brain-size normalized WMH burden values (in cubic centimeters, $cm^3$) per clinical category in each ROI are summarized in demographic Table 1.2 for the NIFD cohort. Participant ages ranged from 45 to 90 years old. Given differences in imaging parameters, whole-brain WMH burden means were lower for categories in the NIFD cohort: CU_NIFD (1.6±2.8 $cm^3$) and FTD_NIFD (2.5±2.9 $cm^3$).

**Table 1.2** Demographic characteristics and WMH volumes (brain-size normalized and adjusted for AT-size values in cubic centimeters) for the NIFD participants used in this study, per clinical category. Participants from a total of two clinical categories were included.

| | N | | | | WMH burden per region of interest (cm3) | | | | | | | | | |
|---|---|---|---|---|---|---|---|---|---|---|---|---|---|---|
| | Total | F | M | Age | Total | ACA | MCA | PCA | LACA | LMCA | LPCA | RACA | RMCA | RPCA |
| Diagnosis | | | | | M ± SD | M ± SD | M ± SD | M ± SD | M ± SD | M ± SD | M ± SD | M ± SD | M ± SD | M ± SD |
| CU | 96 | 53 | 43 | 63.2 ± 7.11 | 1.5993 ± 2.8365 | 0.5463 ± 1.064 | 0.8276 ± 1.6641 | 0.2254 ± 0.2956 | 0.2377 ± 0.5196 | 0.4135 ± 0.8588 | 0.1088 ± 0.1793 | 0.3086 ± 0.5752 | 0.4141 ± 0.8316 | 0.1167 ± 0.1322 |
| FTD | 98 | 46 | 52 | 62.7 ± 7.34 | 2.4739 ± 2.8646 | 1.1497 ± 1.6185 | 1.0029 ± 1.2041 | 0.3214 ± 0.3129 | 0.5983 ± 0.8664 | 0.5186 ± 0.6426 | 0.1527 ± 0.1712 | 0.5513 ± 0.7776 | 0.4843 ± 0.5949 | 0.1686 ± 0.1995 |

### 3.2 Pairwise Comparisons Across Arterial-territories (Aim 1)

#### *3.2.1 AT-specific WMH burden findings – CCNA COMPASS-ND cohort*

All clinical categories exhibited a higher WMH burden in the $MCA_t$ when compared to $ACA_t$ and $PCA_t$, despite correcting for AT size differences. However, when comparing the $ACA_t$ to the $PCA_t$, our analysis unveiled distinct patterns of WMH burden across clinical categories. Specifically, CU, MCI, AD, and PD displayed a higher WMH burden in $PCA_t$ compared to $ACA_t$. Clinical categories characterized by high vascular brain injury (i.e., MCI+V and AD+V) demonstrated a higher WMH burden in $ACA_t$ compared to $PCA_t$ (Fig. 2).

Left and right asymmetry analyses revealed that most categories (6/10, CU, SCD, MCI+V, AD+V, PD, PDD) demonstrated AT-specific asymmetry in the $MCA_t$, with a higher WMH burden on the left side. Additionally, MCI+V and CU had a higher WMH burden in the $RACA_t$ and MCI+V, AD, and PDD had a higher WMH burden in the $RPCA_t$ (Fig. 2).

***SCD***

Note that we report on SCD findings separately, given that this group differs from controls only due to subjective self-reported cognitive impairment, with no objective impairment detected in cognitive testing. Similar to the other clinical categories, SCD demonstrated a higher WMH burden in the $MCA_t$ relative to both the $ACA_t$ and $PCA_t$ (Fig. 2). However, no significant difference was detected between the $ACA_t$ and $PCA_t$ (Fig. 2). Within the $MCA_t$, an asymmetry in burden distribution was observed, with the $LMCA_t$ displaying a higher WMH burden than the $RMCA_t$.

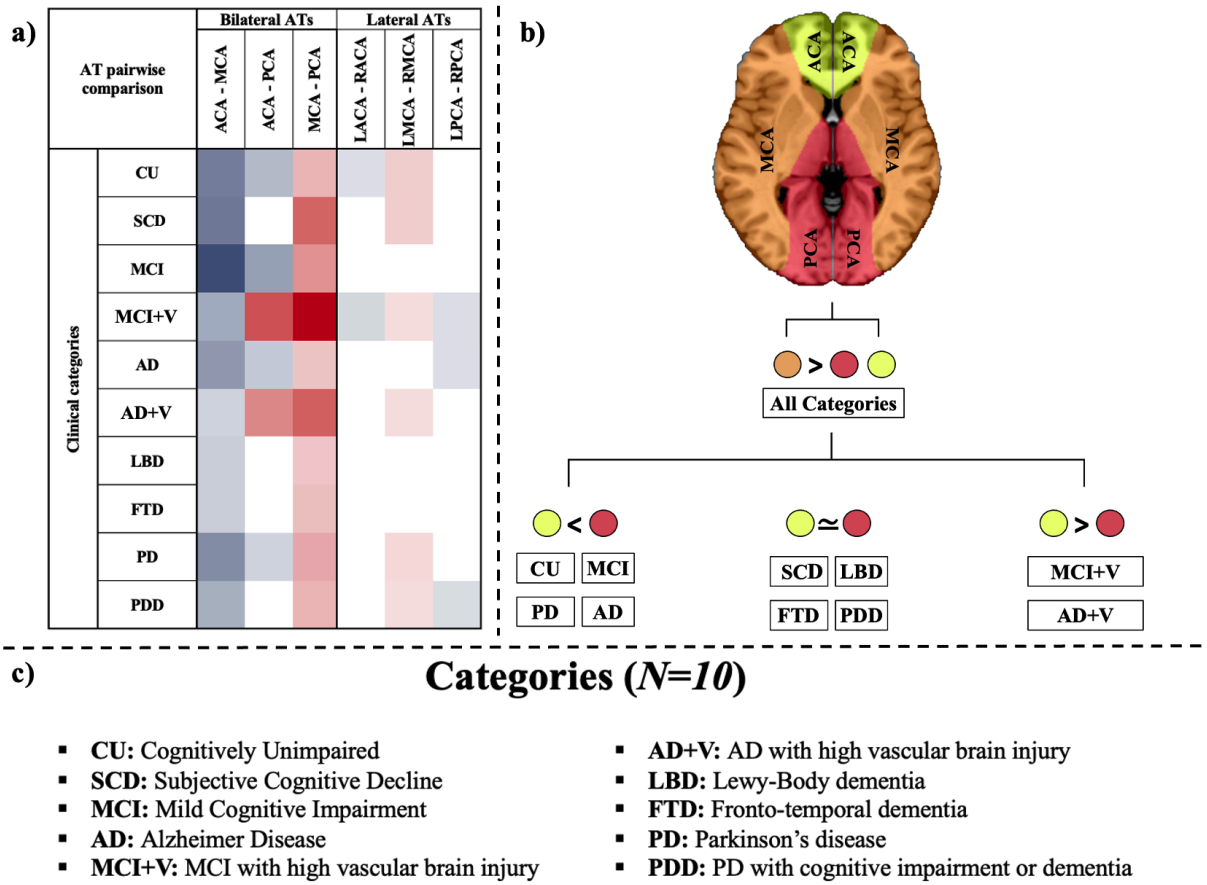


**Fig. 2.** *AT-specific WMH comparisons between regions.* **a)** Columns indicate pairs of contrasted regions (AT 1 - AT 2), each row referring to a distinct clinical category. The red color represents regions where AT 1 has a significantly *higher* WMH burden than AT 2, with the intensity representing *t*-values. Similarly, the blue color represents regions where AT 1 has a significantly *lower* WMH-metric than AT 2. White cells represent contrasts that exhibit no significant statistical difference. Results are corrected for multiple comparisons using FDR. **b)** Altered visualization for the bilateral ATs section of Fig. 2a, where each color represents a different AT. The mathematical comparative signs indicate the differences in WMH burden between these ATs for each clinical group. **c)** Acronym definition for the ten presented CCNA COMPASS-ND categories.

### *3.2.2 AT-specific WMH burden findings – NIFD cohort*

Consistent with our FTD findings in the CCNA COMPASS-ND cohort, FTD_NIFD had a higher WMH burden in the $MCA_t$ compared to the other ATs. However, FTD_NIFD had a higher WMH burden in the $ACA_t$ than in the $PCA_t$ (Supplemental Fig. 1), while no significant difference between the $ACA_t$ and $PCA_t$ was detected in FTD (CCNA COMPASS-ND). Consistent with our CCNA COMPASS-ND findings, the FTD_NIFD cohort showed no asymmetry.

### 3.3 Pairwise Comparisons Across Clinical Categories (Aim 2) (WMH burden)

#### *3.3.1 WMH burden findings – CCNA COMPASS-ND cohort*

The results of pairwise group comparisons for whole-brain (or total) and regional WMH burden are summarized in Fig. 3a. The number of categories for which a given group had a higher WMH burden in a specific region are indicated in Fig. 3b. These values are alternatively visualized in the frequency histogram shown in Fig. 3c.

**Whole-brain findings:** Pairwise comparisons between clinical categories found those characterized by a high vascular brain injury (i.e., MCI+V and AD+V) to have a significantly higher whole-brain WMH burden compared to all non-vascular clinical categories, except FTD (Fig. 3). In the non-vascular clinical categories, FTD had a significantly higher whole-brain WMH burden, except when compared to LBD. Of the remaining six clinical categories, LBD, AD, and PDD had a significantly higher whole-brain WMH burden compared to PD, MCI, and CU (Fig. 3).

**AT-specific findings:** In the $ACA_t$ and $MCA_t$, WMH burden pairwise comparisons between clinical categories were consistent with whole-brain findings, except for AD, which was not significantly different from PD (Fig. 3). Pairwise comparisons in the $MCA_t$ showed two additional group differences in WMH burden that were not detected when looking at the whole-brain, namely, FTD higher than LBD and PD higher than CU (Fig. 3). Pairwise comparisons between clinical categories in the $PCA_t$ showed fewer group differences compared to whole-brain findings, with no significant difference detected between (i) MCI+V versus AD, LBD, or PDD, (ii) FTD versus AD or PDD, and (iii) AD+V versus LBD (Fig. 3).

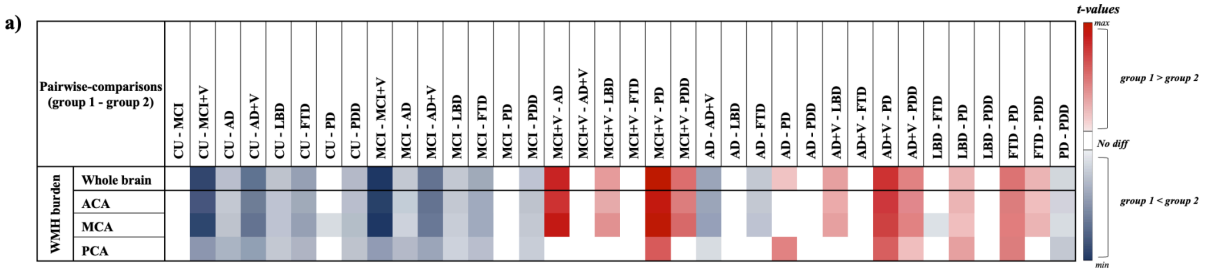


b)

| | Regions of Interest (ROIs) | | | | |
|---|---|---|---|---|---|
| Diagnosis | Whole brain | ACA | MCA | PCA | TOTAL |
| CU | 0 | 0 | 0 | 0 | **0** |
| MCI | 0 | 0 | 0 | 0 | **0** |
| MCI+V | 6 | 6 | 6 | 3 | **21** |
| AD | 3 | 2 | 2 | 3 | **10** |
| AD+V | 6 | 6 | 6 | 5 | **23** |
| LBD | 3 | 3 | 3 | 3 | **12** |
| FTD | 5 | 5 | 6 | 3 | **19** |
| PD | 0 | 0 | 1 | 0 | **1** |
| PDD | 3 | 3 | 3 | 3 | **12** |

*Values represent the number of clinical categories compared to which the row category exhibits a higher WMH burden*

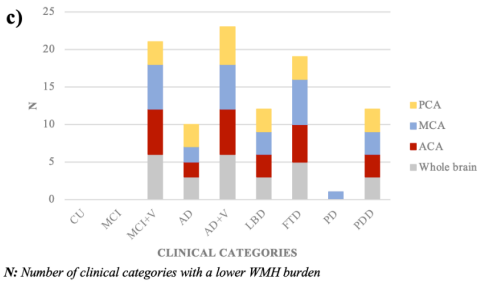


*N: Number of clinical categories with a lower WMH burden*

**Fig. 3.** *AT-specific WMH burden comparisons between clinical categories.* **a)** Columns indicate pairs of contrasted groups (group 1 - group 2), each row referring to a distinct region. The red color represents regions where group 1 has a significantly higher WMH burden than group 2, with the gradient representing *t*-values. Similarly, the blue color represents regions where group 1 has a significantly lower WMH burden than group 2. White cells represent contrasts that exhibit no significant statistical difference. Results are corrected for multiple comparisons using FDR. **b)** Figure summarizes group comparison findings in Fig. 3a. Rows represent specific groups, columns represent ATs, and values indicate the frequency of each group having a higher WMH burden compared to others. **c)** Histogram visualization of findings in Fig. 3b.

## ***SCD***

**Whole-brain findings:** Pairwise comparisons between SCD and other clinical categories showed that SCD exhibited a whole-brain WMH burden that was (i) higher compared to CU and (ii) lower compared to high vascular injury burden categories (MCI+V and AD+V), and dementia categories (AD, LBD, FTD, and PDD) (see Supplemental Fig. 2).

**AT-specific findings:** In the $ACA_t$ and $MCA_t$, WMH burden pairwise comparisons between SCD and other clinical categories were consistent with whole-brain findings, except when compared to AD (see Supplemental Fig. 2). Moreover, SCD had a lower WMH burden in the $PCA_t$ compared to MCI and AD.

### *3.3.2 WMH burden findings – NIFD cohort*

When comparing CU_NIFD and FTD_NIFD cohorts, our WMH burden findings mostly reproduced our CCNA COMPASS-ND CU-FTD comparative findings (i.e., higher WMH burden in FTD across all bilateral and lateral ATs compared to CU). The only exception was

the $RPCA_t$ WMH burden, where no statistically significant difference was detected between CU_NIFD and FTD_NIFD groups (Supplemental Fig. 1).

### *3.3.3 WMH ratio findings – CCNA COMPASS-ND cohort*

The results of pairwise group comparisons for regional WMH ratio are summarized in Fig. 4a. The number of categories for which a given group had a higher WMH ratio in a specific region are indicated in Fig. 4b. These values are alternatively visualized in the frequency histogram shown in Fig. 4c.

WMH ratio pairwise comparisons between clinical categories (N=45) showed that most group differences were detected in the $PCA_t$ (N=19), followed by the $ACA_t$ (N=15) and the $MCA_t$ (N=6) (Fig. 4). Our findings highlighted a contrasting relationship between the $ACA_t$ and $PCA_t$: in most cases (N=13; 62%), when the WMH ratio was lower in the $ACA_t$ it was higher in the $PCA_t$, and vice-versa (Fig. 4).

Categories with a high vascular brain injury (i.e., MCI+V and AD+V) had significantly (i) higher WMH ratio in the $ACA_t$ compared to all other categories, except for LBD and FTD where no difference was detected, and (ii) lower WMH ratio in the $PCA_t$ compared to all other categories, except for FTD where no difference was detected when compared to AD+V (Fig. 4). Only MCI+V had a higher WMH ratio in the $MCA_t$ than all categories, except for FTD and PD. As for the remaining categories, FTD had a WMH ratio that was higher in the $ACA_t$ and lower in the $PCA_t$ compared to AD, MCI, and CU (Fig. 4). PD had a WMH ratio that was (i) lower in the $PCA_t$ compared to AD, MCI, and CU (similar to FTD), and (ii) higher in the $MCA_t$ compared to AD (Fig. 4). Finally, MCI had a higher WMH ratio than LBD, FTD, and PDD in the $ACA_t$.

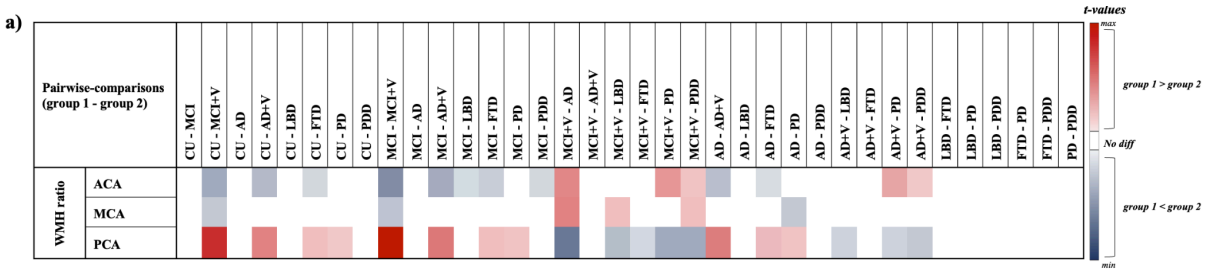


b)

| Diagnosis | Regions of Interest (ROIs) ACA | MCA | PCA | TOTAL |
|---|---|---|---|---|
| CU | 0 | 0 | 4 | **4** |
| MCI | 0 | 0 | 4 | **4** |
| MCI+V | 5 | 5 | 0 | **10** |
| AD | 0 | 0 | 4 | **4** |
| AD+V | 5 | 0 | 0 | **5** |
| LBD | 1 | 0 | 2 | **3** |
| FTD | 3 | 0 | 1 | **4** |
| PD | 0 | 1 | 2 | **3** |
| PDD | 1 | 0 | 2 | **3** |

*Values represent the number of clinical categories compared to which the row category exhibits a higher WMH ratio*

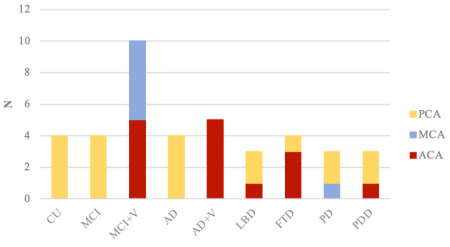


***N:*** *Number of clinical categories with a lower WMH ratio*

***Fig. 4.*** AT-specific WMH ratio comparisons between clinical categories. **a)** Columns indicate pairs of contrasted groups (group 1 - group 2), each row referring to a distinct AT. The red color represents regions where group 1 has a significantly higher WMH ratio than group 2, with the gradient representing t-values. Similarly, the blue color represents regions where group 1 has a significantly lower WMH ratio than group 2. White cells represent contrasts that exhibit no significant statistical difference. Results are corrected for multiple comparisons using FDR. **b)** Figure summarizes group comparison findings in Fig. 4a. Rows represent specific groups, columns represent ATs, and values indicate the frequency of each group having a higher WMH burden compared to others. **c)** Histogram visualization of findings in Fig. 4b.

## ***SCD***

The results of pairwise group comparisons for regional WMH ratio are summarized in Supplemental Fig. 3. Compared to categories with a high vascular injury burden, SCD had a lower $ACA_t$ WMH ratio and a higher $PCA_t$ WMH ratio. SCD had a higher $MCA_t$ WMH ratio and a lower $PCA_t$ WMH ratio than CU, MCI, and AD. Lastly, SCD had a higher $ACA_t$ WMH ratio than MCI.

### *3.3.4 WMH ratio findings – NIFD cohort*

When comparing CU_NIFD and FTD_NIFD cohorts, our WMH ratio findings when comparing CU and FTD (CCNA COMPASS-ND) were not reproduced (i.e., higher WMH ratio than CU in the $ACA_t$ and lower in the $PCA_t$). The NIFD cohort showed no statistically significant WMH ratio differences between CU_NIFD and FTD_NIFD (Supplemental Fig. 1).

### 3.4 Sex Analysis – WMH burden and Ratio (Aim 3)

Compared to women, men exhibited higher whole-brain and $MCA_t$ WMH burden in CU, MCI+V, and FTD. Additionally, men showed a higher $ACA_t$ WMH burden than women in MCI+V, as well as a higher $PCA_t$ WMH burden in MCI, FTD, and PD (Table 2.1). In terms of the WMH ratio analyses, women exhibited a higher $ACA_t$ WMH ratio in SCD and $MCA_t$ and a lower $MCA_t$ WMH ratio in PDD (Table 2.2).

**Table 2.1.** WMH burden Sex-analyses

Negative *t*-values represent instances where men had a lower WMH burden, and vice versa for positive *t*-values. Statistically significant findings after FDR correction are shown in bold.

| | | | | | ROIs (N=10) | | | | | |
|---|---|---|---|---|---|---|---|---|---|---|
| Cohorts | Whole brain | ACA | MCA | PCA | LACA | LMCA | LPCA | RACA | RMCA | RPCA |
| | *t* , *p* | *t* , *p* | *t* , *p* | *t* , *p* | *t* , *p* | *t* , *p* | *t* , *p* | *t* , *p* | *t* , *p* | *t* , *p* |
| CU | **2.02 , 0.05** | 1.70 , 0.09 | **2.31 , 0.02** | 1.02 , 0.31 | 1.19 , 0.24 | 1.90 , 0.06 | 0.81 , 0.42 | 1.74 , 0.08 | **2.61 , 0.01** | 1.10 , 0.28 |
| SCD | -0.11 , 0.91 | -1.11 , 0.27 | 0.27 , 0.79 | 0.78 , 0.44 | -0.93 , 0.36 | 0.42 , 0.68 | 0.33 , 0.74 | -1.18 , 0.24 | 0.19 , 0.85 | 1.12 , 0.27 |
| MCI | 0.77 , 0.44 | -0.51 , 0.61 | 0.75 , 0.45 | **2.27 , 0.02** | -0.82 , 0.41 | 0.46 , 0.65 | **2.24 , 0.03** | -0.69 , 0.49 | 1.07 , 0.29 | **2.01 , 0.05** |
| MCI+V | **2.22 , 0.03** | **2.20 , 0.03** | **2.17 , 0.03** | 1.79 , 0.08 | **2.28 , 0.02** | **2.18 , 0.03** | **2.06 , 0.04** | **2.07 , 0.04** | **2.07 , 0.04** | 1.32 , 0.19 |
| AD | -0.82 , 0.41 | -1.13 , 0.26 | -0.63 , 0.53 | -0.34 , 0.74 | -1.51 , 0.14 | -0.79 , 0.43 | -1.24 , 0.22 | -0.79 , 0.43 | -0.44 , 0.66 | 0.24 , 0.81 |
| AD+V | 0.76 , 0.45 | 0.71 , 0.48 | 0.58 , 0.57 | 1.00 , 0.32 | 0.33 , 0.75 | 0.25 , 0.80 | 1.00 , 0.32 | 1.02 , 0.31 | 0.82 , 0.42 | 0.65 , 0.52 |
| LBD | 0.58 , 0.57 | 0.11 , 0.91 | 0.68 , 0.50 | 0.92 , 0.37 | -0.06 , 0.95 | 0.66 , 0.52 | 0.98 , 0.34 | 0.13 , 0.90 | 0.61 , 0.54 | 0.67 , 0.51 |
| FTD | **2.79 , 0.01** | 2.00 , 0.06 | **2.81 , 0.01** | **3.45 , 0.00** | 1.66 , 0.11 | **2.29 , 0.03** | **2.85 , 0.01** | **2.18 , 0.04** | **2.80 , 0.01** | **3.50 , 0.00** |
| PD | 1.13 , 0.26 | 0.24 , 0.81 | 1.12 , 0.27 | **2.50 , 0.01** | 0.36 , 0.72 | 1.02 , 0.31 | 1.85 , 0.07 | 0.03 , 0.98 | 1.21 , 0.23 | **2.61 , 0.01** |
| PDD | 0.49 , 0.62 | 0.00 , 1.00 | 0.79 , 0.43 | -0.04 , 0.97 | -0.20 , 0.84 | 0.78 , 0.44 | 0.11 , 0.91 | 0.19 , 0.85 | 0.74 , 0.46 | -0.22 , 0.83 |

**Table 2.2.** WMH ratio Sex-analyses

Negative *t*-values represent instances where men had a lower WMH ratio, and vice versa for positive *t*-values. Statistically significant findings after FDR correction are shown in bold.

| | | | | | ROIs (N=10) | | | | |
|---|---|---|---|---|---|---|---|---|---|
| Cohorts | ACA | MCA | PCA | LACA | LMCA | LPCA | RACA | RMCA | RPCA |
| | *t* , *p* | *t* , *p* | *t* , *p* | *t* , *p* | *t* , *p* | *t* , *p* | *t* , *p* | *t* , *p* | *t* , *p* |
| CU | 0.39 , 0.69 | 1.49 , 0.14 | -1.25 , 0.21 | -0.40 , 0.69 | 0.33 , 0.74 | -1.29 , 0.20 | 0.54 , 0.59 | **2.06 , 0.04** | -0.88 , 0.38 |
| SCD | **-2.48 , 0.01** | 1.36 , 0.18 | 1.27 , 0.21 | -1.51 , 0.13 | 1.33 , 0.19 | 0.61 , 0.54 | **-2.20 , 0.03** | 0.84 , 0.40 | 1.65 , 0.10 |
| MCI | **-2.24 , 0.03** | -0.75 , 0.45 | 1.85 , 0.07 | **-2.65 , 0.01** | -1.30 , 0.20 | 1.76 , 0.08 | -1.17 , 0.24 | 0.29 , 0.78 | 1.45 , 0.15 |
| MCI+V | 1.65 , 0.10 | -0.28 , 0.78 | -0.88 , 0.38 | 1.73 , 0.09 | -0.12 , 0.91 | -0.41 , 0.69 | 1.22 , 0.22 | -0.29 , 0.77 | -1.10 , 0.27 |
| AD | -1.27 , 0.21 | 0.56 , 0.58 | 0.81 , 0.42 | -1.83 , 0.07 | 0.00 , 1.00 | -0.65 , 0.52 | -0.46 , 0.65 | 0.85 , 0.39 | 1.64 , 0.11 |
| AD+V | 0.26 , 0.80 | -1.09 , 0.28 | 0.05 , 0.96 | -0.57 , 0.57 | -1.80 , 0.08 | 0.28 , 0.78 | 0.88 , 0.38 | -0.09 , 0.93 | -0.32 , 0.75 |
| LBD | -1.03 , 0.31 | 0.66 , 0.52 | 0.55 , 0.59 | -1.00 , 0.33 | 0.51 , 0.62 | 0.32 , 0.75 | -0.78 , 0.44 | 0.29 , 0.78 | 0.35 , 0.73 |
| FTD | -0.19 , 0.85 | -0.14 , 0.89 | 0.08 , 0.94 | -0.32 , 0.75 | -0.90 , 0.38 | -0.08 , 0.94 | 0.14 , 0.89 | 0.26 , 0.80 | 0.23 , 0.82 |
| PD | -1.93 , 0.06 | -0.27 , 0.79 | 1.36 , 0.18 | -1.38 , 0.17 | -0.44 , 0.66 | 0.49 , 0.63 | -1.86 , 0.07 | 0.15 , 0.88 | 1.62 , 0.11 |
| PD | -0.81 , 0.42 | **2.36 , 0.02** | -0.64 , 0.52 | -1.25 , 0.22 | 1.86 , 0.07 | -0.38 , 0.71 | -0.11 , 0.91 | 1.72 , 0.09 | -0.84 , 0.41 |

### 3.5 Association Between AT-specific WMH burden and Cognition (Aim 4)

#### *3.5.1 Analysis independent of diagnosis (Aim 4.1)*

Our results revealed that, when adjusting for clinical diagnosis: (i) SRT scores were associated with ACA WMH burden ($p$=0.002; $t$=2.44), (ii) CRT and MoCA scores were associated with PCA WMH burden (CRT: $p$=0.002; $t$=2.40 | MoCA: $p$=0.001; $t$=-3.21), and (iii) DSST scores were associated with WMH burden across all ATs (PCA: $p$<0.001; $t$=-3.96 | MCA: $p$=0.004; $t$=-2.83 | ACA: $p$=0.02; $t$=-2.26).

### *3.5.2 NDD-specific analysis (Aim 4.2)*

MCI and AD were the only categories to exhibit AT-specific WMH burden associations with cognitive performance (Fig. 5c). In MCI, lower DSST scores were associated with higher PCA WMH burden ($p$=0.02; $t$=-2.78) (Fig. 5d). In AD, a lower percentage of correct answers in CRT tasks was associated with higher ACA ($p$=0.006; $t$=-3.32) and MCA ($p$=0.02; $t$=-2.59) WMH burden (Fig. 5e).

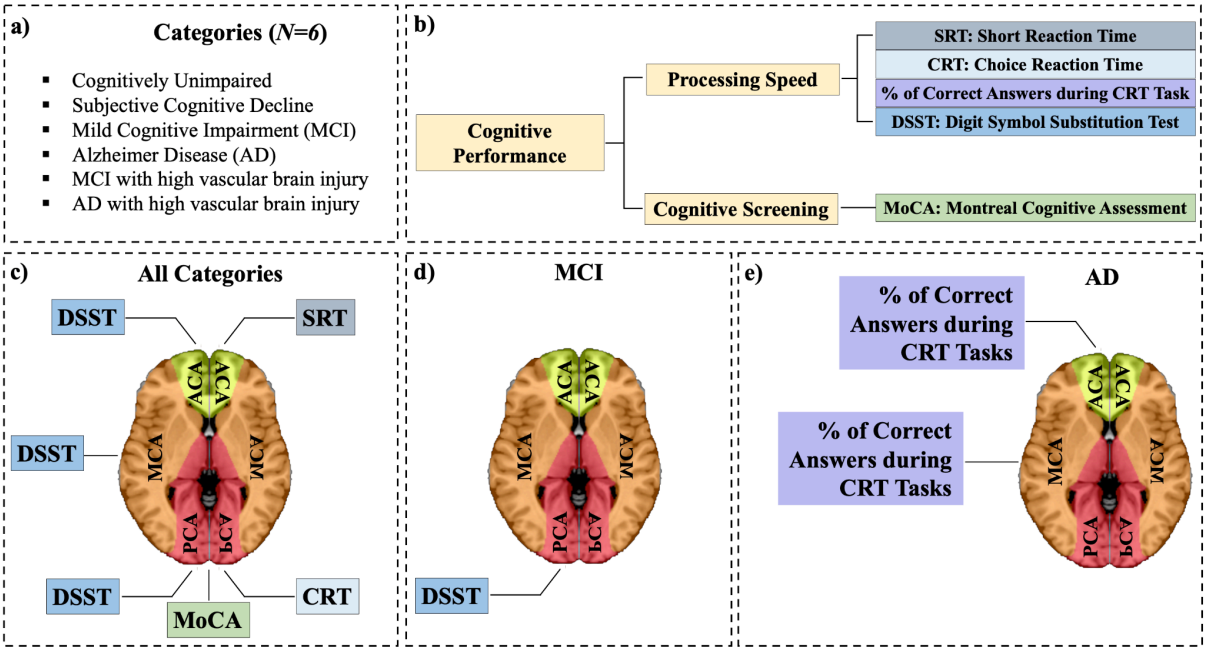


***Fig. 5.*** *Associations between AT-specific WMH burden and Cognitive Performance* **a)** Clinical categories analyzed. **b)** Tasks used for cognitive assessment. **c)** Across categories analysis: AT-specific WMH burden associations with cognitive scores from different cognitive assessments. **d)** NDD-specific analysis: PCA WMH burden was associated with DSST scores in MCI. **e)** NDD-specific analysis: ACA and MCA WMH burden were significantly associated with the percentage of Correct Answers in CRT Tasks in AD. Note: All presented results maintain significance ($p$<0.05) after correcting for multiple comparisons.

## 4. DISCUSSION

In this study, we mapped WMH across ATs associated with the three major cerebral arteries (ACA, MCA, PCA) in both hemispheres in ten clinical categories, uncovering unique AT-specific WMH signatures in certain NDDs and their prodromes. These major cerebral arteries originate from the Circle of Willis [64], with the ACA and MCA supplied by the anterior circulation and the PCA by the posterior circulation. They serve distinct brain

regions: the ACA irrigates the medial hemispheres and superior frontal/parietal lobes; the MCA covers the inferior frontal, inferolateral parietal, and lateral temporal lobes; and the PCA supplies the occipital and medial temporal lobes [65]. Pathological changes in these arteries can lead to AT-specific disturbances and increased WMH burden [31,32].

### 4.1 Insights From WMH burden Distributions Across and Within ATs

#### *4.1.1 Higher $MCA_t$ vulnerability and distinct AT patterns across clinical categories*

Our transdiagnostic investigation of WMH burden differences across bilateral ATs ($MCA_t$, $ACA_t$, $PCA_t$) led to two main conclusions.

First, we found that the $MCA_t$ demonstrated the highest WMH burden across all clinical categories assessed, even after adjusting for territory size. Consistent with our finding, the $MCA_t$ has been reported to have a higher burden of cerebrovascular pathologies compared to other ATs, including infarcts [46,66–70], atherosclerosis [71,72] and WMH [46]. This may be because the MCA is the cerebral artery most frequently affected by pathology [73,74], partly due to the higher hemodynamic-stress associated with its geometry (e.g., diameter, bifurcation angle) and other attributes [75,76]. An example of the latter is that the MCA exhibits the highest sensitivity to blood pressure variations among the anterior circulation arteries [77], an established risk--factor for WMH and other cerebrovascular pathologies [77,78].

Second, our $ACA_t$-$PCA_t$ comparisons revealed AT-specific WMH burden patterns unique to clinical categories with similar whole-brain WMH burden. Specifically, categories with whole-brain WMH volumes of <15 $cm^3$ (CU, AD continuum, PD) exhibited higher WMH burden in the $PCA_t$ compared to the $ACA_t$. Conversely, in clinically recognized high vascular injury categories, namely MCI+V and AD+V with whole-brain WMH volumes of >29 $cm^3$, the WMH burden was higher in the $ACA_t$ than in the $PCA_t$.

Supporting our $ACA_t$-$PCA_t$ findings in the AD continuum, studies have consistently reported an increased posterior WMH burden in these categories [11,43,79–82]. This posterior predominance of WMH in AD is thought to stem from a combination of amyloid pathology [43,83–85] and cerebrovascular issues [86–88]. The main mechanisms include (i) amyloidosis-associated neuroinflammation commencing in the posterior white matter [89,90], (ii) increasing cerebral amyloid angiopathy-associated ischemic injury predominantly

affecting posterior brain vessels, partly due to differential aging of the posterior circulation (e.g., increased collagen content) [35,83,91–94], and (iii) higher frequency of severe PCA occlusion by atherosclerotic lesions [95]. Compared to AD, there are relatively few studies elucidating our $ACA_t$-$PCA_t$ findings in CU and PD. In CU, our findings are supported by a large sample-size study, showing that posterior WMH burden increased more rapidly than in anterior regions [96]. In PD, vascular pathology is increasingly recognized as a contributor to disease pathophysiology, potentially sustaining or exacerbating neuronal degeneration in posterior regions [97]. Additionally, the substantia nigra, which is particularly affected in PD [98,99] is vascularized by the posterior circulation through the PCA and basilar artery [99].

Supporting our $ACA_t$-$PCA_t$ findings, the increased anterior WMH burden observed in the high vascular injury categories (MCI+V, AD+V) aligns with studies reporting that individuals with vascular cognitive impairment and dementia have a higher proportion of the total WMH burden accumulating in the anterior relative to posterior regions [100]. Studies also indicate that (i) more vascular risk-factors (e.g., age, hypertension) are associated with anterior (e.g., $ACA_t$ [46]) than with posterior WMH burden [11,46,80,85], and (ii) early myelin changes in small vessel disease initially involve the frontal lobe, followed by gradual involvement of the parietal, temporal, and occipital lobes [101].

Among the two FTD cohorts investigated, the NIFD cohort exhibited a higher WMH burden in the $ACA_t$ compared to the $PCA_t$, although this difference was not significant in the smaller CCNA cohort. While FTD mostly affects both the frontal and temporal lobes [102–104], our findings align with previous research indicating greater hypoperfusion in the frontal compared to the temporal lobe in FTD [105]. This is particularly relevant as the frontal lobe is largely supplied by the ACA [106], which may explain the observed higher WMH burden in the $ACA_t$. Notably, progranulin mutations, present in 10-20% of the FTD population [107,108] and known to exacerbate WMH burden [109], are primarily linked to glial dysfunction [110]. However, growing evidence suggests that cerebrovascular factors may also play a role in WMH development in both genetic and sporadic forms of the disease. This is supported by findings that (i) progranulin influences vascular tone [111,112], and that progranulin-deficient mice exhibit microvascular alterations in the brain [113] and (ii) hypoperfusion in sporadic FTD leads to the degeneration of a subset of astrocytes [114].

#### *4.1.2 Left-sided hemispheric dominance in WMH burden across clinical categories*

Our transdiagnostic investigation of WMH burden differences within ATs identified hemispheric asymmetries in seven clinical categories (CU, SCD, MCI+V, AD, AD+V, PD, PDD), with 86% showing higher WMH burden in the $LMCA_t$. Hemispheric asymmetries in cerebrovascular properties (e.g., morphology, hemodynamics) contribute to the regional occurrence of vascular pathologies [115], which can increase the ipsilateral WMH burden [116,117]. Emerging literature indicates that the MCA exhibits strong left-sided arterial dominance from the neonatal stage, based on metrics of geometry and hemodynamics [115,118,119]. This early asymmetric blood flow weakens LMCA vascular endothelial functions [115], contributing to the prevalence of left-sided MCA injuries [115,118–120], such as the higher WMH burden we observed. NDD-specific brain hemispheric asymmetry may also play an additive or independent role [121].

### 4.2 Insights From AT-specific WMH metrics Across Clinical Categories

#### *4.2.1 Advantage of using both burden and ratio metrics*

We found that the majority of WMH burden comparisons (36/45; 80%) between clinical categories showed findings in the ATs that followed the whole-brain pattern – for example, compared to MCI, MCI+V had a higher WMH burden in the whole-brain, as well as in all three ATs. Adjusting for the whole-brain WMH burden (i.e., WMH ratio metric) allowed us to uncover additional characteristics of WMH distribution across ATs per clinical category, independent of overall WMH burden. For example, compared to MCI, MCI+V had a higher $ACA_t$ and a lower $PCA_t$ WMH ratio.

#### *4.2.2 AT-specific WMH distribution in CU: Insights from cross-clinical comparisons*

We found that CU consistently exhibited a lower WMH burden across ATs compared to the dementias (AD, AD+V, FTD, LBD, PDD), although the difference with MCI did not reach statistical significance. Despite the limited AT-specific studies in the literature, our findings align with broader research on whole-brain and regional WMH burden in AD and FTD. Specifically, individuals with AD demonstrated greater WMH accumulation both globally and regionally compared to CU [79,81,122,123]. Our AD+V (and MCI+V) findings align with studies that have established a significant association between WMH increase and mixed dementia [16,124–126]. Additionally, FTD individuals, particularly those with the progranulin mutation, typically have a higher WMH burden than CU [127,128]. Although

progranulin status was not available, some of our participants may carry this mutation, as it occurs in 10-20% of the FTD population [107,108]. In contrast to AD and FTD, there exists a lack of consensus in the literature regarding WMH burden in LBD and PDD. Earlier studies reported no significant difference in WMH burden severity relative to CU [122], while recent studies indicate a significantly more severe burden in LBD [129] and PDD [130]. Finally, with regards to PD, although our findings indicated that the increased WMH burden in PD was more pronounced in the $MCA_t$, lobar studies reported that PD had greater WMH volume in the occipital region compared to controls [131]. Our results further showed no significant difference in whole-brain WMH burden between CU and PD, consistent with the literature [131].

**WMH ratio:** Most clinical categories (SCD, MCI+V, AD+V, FTD, PD) showed at least one regional WMH ratio difference compared to CU, with a consistently lower WMH ratio in the $PCA_t$. This suggests that these categories might accumulate WMH disproportionately across ATs, with relatively less accumulation in the $PCA_t$. Further research is needed to understand why WMH tends to accumulate more in the anterior brain regions in these pathologies compared to normal aging.

### *4.2.3 Proportionate increase in WMH across ATs from MCI to AD*

Our pairwise comparisons of WHM burden revealed that MCI individuals had a lower WMH burden compared to those with AD, both in the whole-brain and across all bilateral and lateral ATs (Fig. 3a; Supplemental Fig. 4). The observed AT WMH burden findings in AD are concordant with increased (i) whole-brain WMH burden and (ii) regional WMH burden extracted using other parcellation schemas (e.g., lobar, deep/periventricular), compared to MCI [26,79,81] as well as CU individuals [79,81,123]. The increased WMH burden in the advanced stage of the AD continuum (i.e., dementia stage) was expected given that cerebrovascular perturbations appear early in the disease course (around the same time as Aβ) in both autosomal and sporadic forms of AD, and progress with the severity of the disease [132–136][87]. Moreover, in sporadic AD, vascular abnormalities have been found to be ~80% more pronounced than other AD biomarkers (e.g., Aβ deposition) from an early stage of the disease, well before clinical onset [135].

While AD had a higher WMH burden than MCI across all ATs, we did not detect any significant WMH ratio findings between the two clinical categories, or when compared to

CU. Our observations align with voxel-based literature findings showing that although MCI and AD had a higher WMH burden than CU, this difference disappeared after adjusting for whole-brain WMH burden [123]. Collectively, our findings suggested a proportionate increase in WMH across the ATs as MCI progresses to AD. However, as our findings were based on cross-sectional data, longitudinal studies are needed to confirm these results.

#### *4.2.4 Absence of differences in AT-specific WMH metrics between MCI+V and AD+V*

We found no significant difference in WMH metrics (whole-brain or AT-specific) between MCI+V and AD+V. Since their diagnostic criteria did not rely solely on WMH burden [137–139], they may exhibit AT-specific differences in other vascular pathologies [140,141], such as microbleeds and infarcts. Although no significant difference in microbleed count was found between the two categories in our CCNA COMPASS-ND cohort [142], we did not explore their AT-specific distributions, as it fell outside the scope of our study. We recommend that future studies address this aspect.

#### *4.2.5 Distinct AT-specific WMH patterns in vascular versus neurodegenerative conditions*

We found that the vascular categories (MCI+V, AD+V) had a higher WMH burden than MCI and AD across all investigated regions, except in the $PCA_t$, where MCI+V and AD had similar burden. The latter finding was not unexpected given that, as previously mentioned (Section 4.1), WMH accumulation in posterior brain regions (including the $PCA_t$) is common in the AD continuum [42], with the greatest burden likely occurring at the dementia stage. We further found that vascular categories displayed a higher WMH ratio in the $ACA_t$ and a lower ratio in the $PCA_t$ when compared to MCI and AD. These findings align with literature indicating that (i) individuals with vascular dementia exhibit more anterior than posterior white matter abnormalities compared to AD [100] and (ii) WMH in posterior brain regions may be secondary to AD pathology (i.e., Aβ) [11,85,143,144], whereas WMH in frontal regions are more strongly associated with vascular risk-factors such as hypertension [11,42,46,80,85].

#### *4.2.6 Contrasting AT-specific WMH metrics between FTD and AD*

FTD is often misdiagnosed as AD or other conditions including psychiatric disorders [145–148]. Given this, it is important to note that we observed distinct differences in AT-based WMH metrics between FTD and AD. Specifically, FTD exhibited a higher WMH burden in the $ACA_t$ and $MCA_t$ regions, along with a higher $ACA_t$ and lower $PCA_t$ WMH

ratio. These findings are consistent with the contrasting spatial patterns observed between FTD and AD using other brain imaging-derived measures, such as hypoperfusion, brain atrophy, and perturbed blood-oxygen-level-dependent (BOLD) signal [149–155]. Our results, combined with existing literature, underscored distinct spatial patterns that could help mitigate the frequent misdiagnosis of FTD as AD [145].

#### *4.2.7 LBD and PDD share similar AT-specific WMH patterns, unlike PD*

PD, PDD, and LBD are characterized by the presence of abnormal alpha-synuclein deposits in Lewy bodies [156,157]. Our results showed no significant differences in WMH burden or ratio between LBD and PDD across all regions. Both LBD and PDD exhibited a higher WMH burden than PD in the whole-brain and bilateral ATs, though WMH ratios were not statistically different. This aligns with literature indicating a greater WMH burden in PDD compared to PD [158,159].

LBD and PDD showed no significant differences in WMH burden or ratios compared to AD, consistent with reports of no overall WMH differences between AD and LBD [160]. In contrast, PD had a lower total WMH burden than AD, particularly in the $PCA_t$, which is often associated with AD-related pathologies (see section 4.1.1).

#### *4.2.8 Distinct AT-specific WMH Patterns in SCD compared to CU and AD continuum*

SCD refers to self-reported worsening of cognitive performance or increasing difficulties with memory and thinking [161]. Individuals with SCD have twice the risk of developing MCI or dementia compared to normal aging individuals [162,163]. Identifying objective metrics that differentiate SCD from normal aging is crucial for early detection. Our findings indicated that SCD had a higher whole-brain WMH burden than CU, particularly in the $ACA_t$ and $MCA_t$, suggesting a distinct WMH profile compared to normal aging. While not all individuals with SCD progress to MCI or AD, longitudinal studies estimate that approximately 20-45% eventually receive such a diagnosis [164–171]. Our results showed that SCD had a significantly lower WMH burden in the $PCA_t$ compared to MCI, though this difference was not observed at the whole-brain level. In comparison to AD, SCD had a significantly lower WMH burden in the $PCA_t$ and at the whole-brain level, suggesting progressive posterior WMH accumulation in AD.

### 4.3 Sex-specific Differences

Sex-specific differences in WMH burden were observed across several clinical categories (Table 2.1). Consistent with literature suggesting that men tend to experience greater cardiovascular risk factor-related differences in total brain volumes than women [172], men were found to have a higher WMH burden in the whole-brain (controlled for brain size via the use of a standardized brain space) and/or an arterial region across several categories (CU, MCI, MCI+V, FTD, PD). However, after controlling for total WMH burden (i.e., using the WMH ratio), women exhibited a higher $ACA_t$ WMH ratio in SCD and MCI (Table 2.2). The literature suggests that in normally aging elderly cohorts, women tended to have a higher proportion of WMH compared to men, relative to the size of their white matter [173–175]. However, this trend may not have been reflected in our findings due to the high proportion of women (80%) in our CU sample, potentially leading to an underrepresentation of WMH distribution in men. Research further reports that women had slower WMH progression with age across the total brain, particularly in the frontal region [176].

### 4.4 Cognition

Cognition results revealed that greater WMH burden was associated with poorer cognitive performance, indicated by higher SRT and CRT scores, as well as lower MoCA scores, DSST scores, and the percentage of correct answers in CRT tasks (see Fig. 5). Mounting evidence suggests that WMH exert an independent effect on cognition in AD, which is additive to the effects of core proteinopathies, such as Aβ and tau [177]. A recent study found that WMH burden in PCA sub-regions contributes to lower cognition, independent of Aβ deposition or atrophy in early AD [11]. Supporting this finding, we observed an association between PCA WMH burden and processing speed at the MCI stage (Fig. 5). However, this association evolved to the ACA and MCA regions at the AD stage (Fig. 5). Since AD is characterized by increased Aβ deposits in areas perfused by the ACA and MCA [178], further investigation is warranted to determine whether the observed associations are driven by WMH or other AD pathologies.

### 4.5 Limitations and Future Directions

Notwithstanding the significant findings, this study is not without its limitations. The ROI-based approach does not allow the detection of regional WMH variations within the ROIs. While it offers advantages in terms of noise robustness and statistical power, considering more fine-grained analyses of WMH could uncover additional insights into their

neuropathological characteristics and implications [26]. Another limitation was the large inter-individual variations in AT-specific WMH, which may reduce the reliability and accuracy of the identified NDD signatures at the individual level. Future work exploring the potential of the NDD signatures characterized in this study to accurately diagnose individuals to their respective clinical categories will be essential. By leveraging advanced deep learning techniques, it could be possible to determine the diagnostic accuracy and generalizability of the identified NDD signatures, potentially paving the way for more effective and precise diagnostic tools in the future. Other future directions include studying our AT-specific findings in conjunction with vascular (e.g., blood pulsatility, arterial density, vessel diameter) and non-vascular (amyloid, tau) features in healthy individuals and different dementia typesSuch an approach would provide insights into the pathophysiology of WMH and their role in the NDDs. Future research is warranted to confirm and expand upon our findings.

## 5. CONCLUSION

Our research underscores the importance of assessing WMH distribution through vascular-based brain parcellation, revealing ATs more susceptible to WMH formation across various NDDs. Understanding these WMH patterns within specific ATs is essential due to their alignment with the brain's vascular architecture and role in NDD pathophysiology. By mapping WMH across ten clinical categories, we provided insights that could help differentiate between disorders. Distinct WMH patterns for several diagnoses suggest that incorporating vascular considerations into imaging criteria may enhance diagnostic precision. While further research is needed, our study lays a strong foundation for integrating vascular insights into diagnostic practices and developing targeted interventions in neurodegeneration.

## 6. ACKNOWLEDGMENTS

This research was funded by Fonds de Recherche Québec – Santé (FRQS) Chercheurs boursiers Junior 1 (2020–2024) and the Fonds de soutien à la recherche pour les neurosciences du vieillissement from the Fondation Courtois (A.B.). We would also like to thank the following organizations for trainee scholarships: VAST Health Research Training Program MSc Scholarship-2022 and Fondation Lemaire and CIMA-Q MSc Scholarship-2023 (I.H); FRQS bourse de formation à la maîtrise (2021) and FRQS bourse de formation au doctorat (2024) (F.E.D.); VAST Health Research Training Program Doctoral Scholarship-2023 (M.S.).

This research used data from CCNA COMPASS-ND, which was supported by a grant from the Canadian Institutes of Health Research (CIHR), with funding contributions from various partner organizations. We would like to thank Randi Pilon for her help with the CCNA-LORIS database. Finally, we are thankful to have received funding from CCNA Team 9 and the CCNA Women Sex Gender Dementia Program.

This research used data from the Frontotemporal Lobar Degeneration Neuroimaging Initiative (FTLDNI also known as NIFD). Data collection and sharing for this project was funded by the Frontotemporal Lobar Degeneration Neuroimaging Initiative (National Institutes of Health Grant R01 AG032306). The study is coordinated through the University of California, San Francisco, Memory and Aging Center. FTLDNI data are disseminated by the Laboratory for Neuro Imaging at the University of Southern California.The investigators at NIFD/FTLDNI contributed to the design and implementation of FTLDNI and/or provided data, but did not participate in analysis or writing of this report. The FTLDNI investigators included the following individuals: Howard Rosen, University of California, San Francisco (PI); Bradford C. Dickerson, Harvard Medical School and Massachusetts General Hospital; Kimoko Domoto-Reilly, University of Washington School of Medicine; David Knopman, Mayo Clinic, Rochester; Bradley F. Boeve, Mayo Clinic Rochester; Adam L. Boxer, University of California, San Francisco; John Kornak, University of California, San Francisco; Bruce L. Miller, University of California, San Francisco; William W. Seeley; University of California, San Francisco; Maria-Luisa Gorno-Tempini, University of California, San Francisco; Scott McGinnis, University of California, San Francisco; Maria Luisa Mandelli, University of California, San Francisco.

## 7. DECLARATION OF INTEREST

S.D. is shareholder and co-founder of True Positive MD Inc. S.N. has received research funding from Roche-Genentech and Immunotec (unrelated to the current work), consulting fees from Sana Biotechnology, and is a part-time employee of NeuroRx Research. All other authors declare having no financial or personal conflicts of interest.

## 8. REFERENCES

[1] Zissimopoulos, J.M., Tysinger, B.C., St Clair, P.A. and Crimmins, E.M. (2018) The Impact of Changes in Population Health and Mortality on Future Prevalence of Alzheimer's Disease and Other Dementias in the United States. *The Journals of Gerontology Series B, Psychological Sciences and Social Sciences*, **73**, S38–47.

[2] Canada, S. (2022) A Portrait of Canada's Growing Population Aged 85 and Older from the 2021 Census.

[3] World Health Organization. (2006) Neurological Disorders: Public Health Challenges. World Health Organization.

[4] Dementia [Internet].

[5] Alzheimer's and dementia [Internet]. Alzheimer's Disease and Dementia.

[6] Volicer, L., McKee, A. and Hewitt, S. (2001) Dementia. *Neurologic Clinics*, **19**, 867–85.

[7] Plassman, B.L., Langa, K.M., Fisher, G.G., Heeringa, S.G., Weir, D.R., Ofstedal, M.B. et al. (2007) Prevalence of dementia in the United States: the aging, demographics, and memory study. *Neuroepidemiology*, **29**, 125–32.

[8] Hu, H.-Y., Ou, Y.-N., Shen, X.-N., Qu, Y., Ma, Y.-H., Wang, Z.-T. et al. (2021) White matter hyperintensities and risks of cognitive impairment and dementia: A systematic review and meta-analysis of 36 prospective studies. *Neuroscience and Biobehavioral Reviews*, **120**, 16–27.

[9] Salvadó, G., Brugulat-Serrat, A., Sudre, C.H., Grau-Rivera, O., Suárez-Calvet, M., Falcon, C. et al. (2019) Spatial patterns of white matter hyperintensities associated with Alzheimer's disease risk factors in a cognitively healthy middle-aged cohort. *Alzheimer's Research & Therapy*, **11**, 12.

[10] Prins, N.D. and Scheltens, P. (2015) White matter hyperintensities, cognitive impairment and dementia: an update. *Nature Reviews Neurology*, **11**, 157–65.

[11] Garnier-Crussard, A., Bougacha, S., Wirth, M., Dautricourt, S., Sherif, S., Landeau, B. et al. (2022) White matter hyperintensity topography in Alzheimer's disease and links to cognition. *Alzheimer's & Dementia: The Journal of the Alzheimer's Association*, **18**, 422–33.

[12] Debette, S., Schilling, S., Duperron, M.-G., Larsson, S.C. and Markus, H.S. (2019) Clinical Significance of Magnetic Resonance Imaging Markers of Vascular Brain Injury: A Systematic Review and Meta-analysis. *JAMA Neurology*, **76**, 81–94.

[13] Wang, R., Laveskog, A., Laukka, E.J., Kalpouzos, G., Bäckman, L., Fratiglioni, L. et al. (2018) MRI load of cerebral microvascular lesions and neurodegeneration, cognitive decline, and dementia. *Neurology*, **91**, e1487–97.

[14] Wardlaw, J.M., Smith, E.E., Biessels, G.J., Cordonnier, C., Fazekas, F., Frayne, R. et al. (2013) Neuroimaging standards for research into small vessel disease and its contribution to ageing and neurodegeneration. *Lancet Neurology*, **12**, 822–38.

[15] Habes, M., Erus, G., Toledo, J.B., Zhang, T., Bryan, N., Launer, L.J. et al. (2016) White matter hyperintensities and imaging patterns of brain ageing in the general population. *Brain: A Journal of Neurology*, **139**, 1164–79.

[16] Debette, S. and Markus, H.S. (2010) The clinical importance of white matter hyperintensities on brain magnetic resonance imaging: systematic review and meta-analysis. *BMJ* , **341**, c3666.

[17] Forsberg, K.M.E., Zhang, Y., Reiners, J., Ander, M., Niedermayer, A., Fang, L. et al. (2018) Endothelial damage, vascular bagging and remodeling of the microvascular bed in human microangiopathy with deep white matter lesions. *Acta Neuropathologica Communications*, **6**, 128.

[18] Poggesi, A., Pasi, M., Pescini, F., Pantoni, L. and Inzitari, D. (2016) Circulating biologic markers of endothelial dysfunction in cerebral small vessel disease: A review. *Journal of Cerebral Blood Flow and Metabolism: Official Journal of the International Society of Cerebral Blood Flow and Metabolism*, **36**, 72–94.

[19] Brickman, A.M., Guzman, V.A., Gonzalez-Castellon, M., Razlighi, Q., Gu, Y., Narkhede, A. et al. (2015) Cerebral autoregulation, beta amyloid, and white matter hyperintensities are interrelated. *Neuroscience Letters*, **592**, 54–8.

[20] Murray, M.E., Vemuri, P., Preboske, G.M., Murphy, M.C., Schweitzer, K.J., Parisi, J.E. et al. (2012) A quantitative postmortem MRI design sensitive to white matter hyperintensity differences and their relationship with underlying pathology. *Journal of Neuropathology and Experimental Neurology*, **71**, 1113–22.

[21] Gouw, A.A., Seewann, A., van der Flier, W.M., Barkhof, F., Rozemuller, A.M., Scheltens, P. et al. (2011) Heterogeneity of small vessel disease: a systematic review of MRI and histopathology correlations. *Journal of Neurology, Neurosurgery, and Psychiatry*, **82**, 126–35.

[22] Fernando, M.S., Simpson, J.E., Matthews, F., Brayne, C., Lewis, C.E., Barber, R. et al. (2006) White matter lesions in an unselected cohort of the elderly: molecular pathology suggests origin from chronic hypoperfusion injury. *Stroke; a Journal of Cerebral Circulation*, **37**, 1391–8.

[23] Fernando, M.S., O'Brien, J.T., Perry, R.H., English, P., Forster, G., McMeekin, W. et al. (2004) Comparison of the pathology of cerebral white matter with post-mortem magnetic resonance imaging (MRI) in the elderly brain: Post-mortem MRI and white matter pathology. *Neuropathology and Applied Neurobiology*, Wiley. **30**, 385–95.

[24] Hassan, A., Hunt, B.J., O'Sullivan, M., Parmar, K., Bamford, J.M., Briley, D. et al. (2003) Markers of endothelial dysfunction in lacunar infarction and ischaemic leukoaraiosis. *Brain: A Journal of Neurology*, **126**, 424–32.

[25] Bernbaum, M., Menon, B.K., Fick, G., Smith, E.E., Goyal, M., Frayne, R. et al. (2015) Reduced blood flow in normal white matter predicts development of leukoaraiosis. *Journal of Cerebral Blood Flow and Metabolism: Official Journal of the International Society of Cerebral Blood Flow and Metabolism*, **35**, 1610–5.

[26] Botz, J., Lohner, V. and Schirmer, M.D. (2023) Spatial patterns of white matter hyperintensities: a systematic review. *Frontiers in Aging Neuroscience*, **15**, 1165324.

[27] Smith, C.D., Johnson, E.S., Van Eldik, L.J., Jicha, G.A., Schmitt, F.A., Nelson, P.T. et al. (2016) Peripheral (deep) but not periventricular MRI white matter hyperintensities are increased in clinical vascular dementia compared to Alzheimer's disease. *Brain and Behavior*, **6**, e00438.

[28] Wahlund, L.O., Basun, H., Almkvist, O., Andersson-Lundman, G., Julin, P. and Sääf, J. (1994) White matter hyperintensities in dementia: does it matter? *Magnetic Resonance Imaging*, **12**, 387–94.

[29] Grey, M.T., Mitterová, K., Gajdoš, M., Uher, R., Klobušiaková, P., Rektorová, I. et al. (2022)

Differential spatial distribution of white matter lesions in Parkinson's and Alzheimer's diseases and cognitive sequelae. *Journal of Neural Transmission* , **129**, 1023–30.

[30] Kandiah, N., Mak, E., Ng, A., Huang, S., Au, W.L., Sitoh, Y.Y. et al. (2013) Cerebral white matter hyperintensity in Parkinson's disease: a major risk factor for mild cognitive impairment. *Parkinsonism & Related Disorders*, **19**, 680–3.

[31] Gutierrez, J., Murray, J., Chon, C. and Morgello, S. (2018) Relationship between brain large artery characteristics and their downstream arterioles. *Journal of Neurovirology*, **24**, 106–12.

[32] Chen, Z., Li, H., Wu, M., Chang, C., Fan, X., Liu, X. et al. (2020) Caliber of Intracranial Arteries as a Marker for Cerebral Small Vessel Disease. *Frontiers in Neurology*, **11**, 558858.

[33] Goeggel Simonetti, B., Rafay, M.F., Chung, M., Lo, W.D., Beslow, L.A., Billinghurst, L.L. et al. (2020) Comparative study of posterior and anterior circulation stroke in childhood: Results from the International Pediatric Stroke Study. *Neurology*, **94**, e337–44.

[34] Kuybu, O., Tadi, P. and Dossani, R.H. (2023) Posterior Cerebral Artery Stroke. StatPearls Publishing.

[35] Roth, W., Morgello, S., Goldman, J., Mohr, J.P., Elkind, M.S.V., Marshall, R.S. et al. (2017) Histopathological Differences Between the Anterior and Posterior Brain Arteries as a Function of Aging. *Stroke; a Journal of Cerebral Circulation*, **48**, 638–44.

[36] Gierthmühlen, J., Allardt, A., Sawade, M., Wasner, G. and Baron, R. (2010) Role of sympathetic nervous system in activity-induced cerebral perfusion. *Journal of Neurology*, **257**, 1798–805.

[37] Luo, J., Bai, X., Tian, Q., Li, L., Wang, T., Xu, R. et al. (2023) Patterns and implications of artery remodeling based on high-resolution vessel wall imaging in symptomatic severe basilar artery stenosis. *Quantitative Imaging in Medicine and Surgery*, **13**, 2098–108.

[38] Finch, C.E. and Shams, S. (2016) Apolipoprotein E and Sex Bias in Cerebrovascular Aging of Men and Mice. *Trends in Neurosciences*, **39**, 625–37.

[39] Tian, J., Shi, J., Smallman, R., Iwatsubo, T. and Mann, D.M.A. (2006) Relationships in Alzheimer's disease between the extent of Abeta deposition in cerebral blood vessel walls, as cerebral amyloid angiopathy, and the amount of cerebrovascular smooth muscle cells and collagen. *Neuropathology and Applied Neurobiology*, **32**, 332–40.

[40] Voigt, S., Amlal, S., Koemans, E.A., Rasing, I., van Etten, E.S., van Zwet, E.W. et al. (2022) Spatial and temporal intracerebral hemorrhage patterns in Dutch-type hereditary cerebral amyloid angiopathy. *International Journal of Stroke: Official Journal of the International Stroke Society*, **17**, 793–8.

[41] Gutierrez, J., Honig, L., Elkind, M.S.V., Mohr, J.P., Goldman, J., Dwork, A.J. et al. (2016) Brain arterial aging and its relationship to Alzheimer dementia. *Neurology*, **86**, 1507–15.

[42] Phuah, C.-L., Chen, Y., Strain, J.F., Yechoor, N., Laurido-Soto, O.J., Ances, B.M. et al. (2022) Association of Data-Driven White Matter Hyperintensity Spatial Signatures With Distinct Cerebral Small Vessel Disease Etiologies. *Neurology*, **99**, e2535–47.

[43] Weaver, N.A., Doeven, T., Barkhof, F., Biesbroek, J.M., Groeneveld, O.N., Kuijf, H.J. et al. (2019) Cerebral amyloid burden is associated with white matter hyperintensity location in specific posterior white matter regions. *Neurobiology of Aging*, **84**, 225–34.

[44] Wen, W. and Sachdev, P. (2004) The topography of white matter hyperintensities on brain MRI in healthy 60- to 64-year-old individuals. *NeuroImage*, **22**, 144–54.

[45] Wen, W. and Sachdev, P.S. (2004) Extent and distribution of white matter hyperintensities in stroke patients: the Sydney Stroke Study. *Stroke; a Journal of Cerebral Circulation*, **35**, 2813–9.

[46] Schirmer, M.D., Giese, A.-K., Fotiadis, P., Etherton, M.R., Cloonan, L., Viswanathan, A. et al. (2019) Spatial Signature of White Matter Hyperintensities in Stroke Patients. *Frontiers in Neurology*, **10**, 208.

[47] Alqarni, A., Jiang, J., Crawford, J.D., Koch, F., Brodaty, H., Sachdev, P. et al. (2021) Sex differences in risk factors for white matter hyperintensities in non-demented older individuals. *Neurobiology of Aging*, Elsevier BV. **98**, 197–204.

[48] Guo, W. and Shi, J. (2022) White matter hyperintensities volume and cognition: A meta-analysis. *Frontiers in Aging Neuroscience*, **14**, 949763.

[49] Chertkow, H., Borrie, M., Whitehead, V., Black, S.E., Feldman, H.H., Gauthier, S. et al. (2019) The Comprehensive Assessment of Neurodegeneration and dementia: Canadian cohort study. *The Canadian Journal of Neurological Sciences Le Journal Canadien Des Sciences Neurologiques*, Cambridge University Press (CUP). **46**, 499–511.

[50] Mohaddes, Z., Das, S., Abou-Haidar, R., Safi-Harab, M., Blader, D., Callegaro, J. et al. (2018) National Neuroinformatics Framework for Canadian Consortium on Neurodegeneration in Aging (CCNA). *Frontiers in Neuroinformatics*, **12**, 85.

[51] Duchesne, S., Chouinard, I., Potvin, O., Fonov, V.S., Khademi, A., Bartha, R. et al. (2019) The Canadian Dementia Imaging Protocol: Harmonizing National Cohorts. *Journal of Magnetic Resonance Imaging: JMRI*, **49**, 456–65.

[52] De Francesco, S., Crema, C., Archetti, D., Muscio, C., Reid, R.I., Nigri, A. et al. (2023) Differential diagnosis of neurodegenerative dementias with the explainable MRI based machine learning algorithm MUQUBIA. *Scientific Reports*, **13**, 17355.

[53] Canadian consortium on neurodegeneration in aging [Internet].

[54] Coupe, P., Yger, P., Prima, S., Hellier, P., Kervrann, C. and Barillot, C. (2008) An optimized blockwise nonlocal means denoising filter for 3-D magnetic resonance images. *IEEE Transactions on Medical Imaging*, **27**, 425–41.

[55] Sled, J.G., Zijdenbos, A.P. and Evans, A.C. (1998) A nonparametric method for automatic correction of intensity nonuniformity in MRI data. *IEEE Transactions on Medical Imaging*, **17**, 87–97.

[56] Dadar, M., Mahmoud, S., Zhernovaia, M., Camicioli, R., Maranzano, J., Duchesne, S. et al. (2022) White matter hyperintensity distribution differences in aging and neurodegenerative disease cohorts. *NeuroImage Clinical*, **36**, 103204.

[57] Dadar, M., Maranzano, J., Misquitta, K., Anor, C.J., Fonov, V.S., Tartaglia, M.C. et al. (2017) Performance comparison of 10 different classification techniques in segmenting white matter hyperintensities in aging. *NeuroImage*, **157**, 233–49.

[58] Dadar, M., Maranzano, J., Ducharme, S., Carmichael, O.T., Decarli, C., Collins, D.L. et al. (2018) Validation of T1w-based segmentations of white matter hyperintensity volumes in large-scale datasets of aging. *Human Brain Mapping*, **39**, 1093–107.

[59] Zahr, N. and Pfefferbaum, A. (2024) Serum albumin and white matter hyperintensities. *Research Square*,. https://doi.org/10.21203/rs.3.rs-3822513/v1

[60] Schmidt, P. (2017) Bayesian inference for structured additive regression models for large-scale

problems with applications to medical imaging [Internet] [Text.PhDThesis]. Ludwig-Maximilians-Universität München.

[61] Yushkevich, P.A., Piven, J., Hazlett, H.C., Smith, R.G., Ho, S., Gee, J.C. et al. (2006) User-guided 3D active contour segmentation of anatomical structures: significantly improved efficiency and reliability. *NeuroImage*, **31**, 1116–28.

[62] Report and Cite Packages [Internet].

[63] Lenth, R.V. (2023) Estimated Marginal Means, aka Least-Squares Means [R package emmeans version 1.8.6]. Comprehensive R Archive Network (CRAN).

[64] Rosner, J., Reddy, V. and Lui, F. (2022) Neuroanatomy, Circle of Willis. *StatPearls*, StatPearls Publishing, Treasure Island (FL).

[65] Loftus, B.D., Athni, S.S. and Cherches, I.M. (2010) CHAPTER 2 - Clinical Neuroanatomy. In: Rolak LA, editor. *Neurology Secrets (Fifth Edition)*, Mosby, Philadelphia. p. 18–54.

[66] Ng, Y.S., Stein, J., Ning, M. and Black-Schaffer, R.M. (2007) Comparison of clinical characteristics and functional outcomes of ischemic stroke in different vascular territories. *Stroke; a Journal of Cerebral Circulation*, **38**, 2309–14.

[67] Nichols, L., Bridgewater, J.C., Wagner, N.B., Karivelil, M., Koelmeyer, H., Goings, D. et al. (2021) Where in the Brain do Strokes Occur? A Pilot Study and Call for Data. *Clinical Medicine & Research*, **19**, 110–5.

[68] Mair, G., White, P., Bath, P.M., Muir, K., Martin, C., Dye, D. et al. (2023) Accuracy of artificial intelligence software for CT angiography in stroke. *Annals of Clinical and Translational Neurology*, **10**, 1072–82.

[69] Abdu, H., Tadese, F. and Seyoum, G. (2021) Comparison of Ischemic and Hemorrhagic Stroke in the Medical Ward of Dessie Referral Hospital, Northeast Ethiopia: A Retrospective Study. *Neurology Research International*, **2021**, 9996958.

[70] Raghavan, S., Graff-Radford, J., Scharf, E., Przybelski, S.A., Lesnick, T.G., Gregg, B. et al. (2021) Study of Symptomatic vs. Silent Brain Infarctions on MRI in Elderly Subjects. *Frontiers in Neurology*, **12**, 615024.

[71] Saba, L., Sanfilippo, R., Porcu, M., Lucatelli, P., Montisci, R., Zaccagna, F. et al. (2017) Relationship between white matter hyperintensities volume and the circle of Willis configurations in patients with carotid artery pathology. *European Journal of Radiology*, **89**, 111–6.

[72] Ritz, K., Denswil, N.P., Stam, O.C.G., van Lieshout, J.J. and Daemen, M.J.A.P. (2014) Cause and mechanisms of intracranial atherosclerosis. *Circulation*, **130**, 1407–14.

[73] Navarro-Orozco, D. and Sánchez-Manso, J.C. (2023) Neuroanatomy, Middle Cerebral Artery. *StatPearls*, StatPearls Publishing, Treasure Island (FL).

[74] Anuradha, H.K., Garg, R.K., Agarwal, A., Sinha, M.K., Verma, R., Singh, M.K. et al. (2010) Predictors of stroke in patients of tuberculous meningitis and its effect on the outcome. *QJM: Monthly Journal of the Association of Physicians*, **103**, 671–8.

[75] Alfano, J.M., Kolega, J., Natarajan, S.K., Xiang, J., Paluch, R.A., Levy, E.I. et al. (2013) Intracranial aneurysms occur more frequently at bifurcation sites that typically experience higher hemodynamic stresses. *Neurosurgery*, **73**, 497–505.

[76] Tan, J., Zhu, H., Huang, J., Ouyang, H.Y., Pan, X., Zhao, Y. et al. (2022) The Association of Morphological Differences of Middle Cerebral Artery Bifurcation and Aneurysm Formation: A Systematic Review and Meta-Analysis. *World Neurosurgery*, **167**, 17–27.

[77] Kizhisseri, M., Gharaie, S., Boopathy, S.R., Lim, R.P., Mohammadzadeh, M. and Schluter, J. (2023) Differential sensitivities to blood pressure variations in internal carotid and intracranial arteries: a numerical approach to stroke prediction. *Scientific Reports*, **13**, 22319.

[78] Koohi, F., Harshfield, E.L. and Markus, H.S. (2023) Contribution of Conventional Cardiovascular Risk Factors to Brain White Matter Hyperintensities. *Journal of the American Heart Association*, **12**, e030676.

[79] Yoshita, M., Fletcher, E., Harvey, D., Ortega, M., Martinez, O., Mungas, D.M. et al. (2006) Extent and distribution of white matter hyperintensities in normal aging, MCI, and AD. *Neurology*, **67**, 2192–8.

[80] Brickman, A.M. (2013) Contemplating Alzheimer's disease and the contribution of white matter hyperintensities. *Current Neurology and Neuroscience Reports*, Springer Science and Business Media LLC. **13**, 415.

[81] Kamal, F., Morrison, C., Maranzano, J., Zeighami, Y. and Dadar, M. (2023) Topographical differences in white matter hyperintensity burden and cognition in aging, MCI, and AD. *GeroScience*, **45**, 1–16.

[82] Brickman, A.M., Zahodne, L.B., Guzman, V.A., Narkhede, A., Meier, I.B., Griffith, E.Y. et al. (2015) Reconsidering harbingers of dementia: progression of parietal lobe white matter hyperintensities predicts Alzheimer's disease incidence. *Neurobiology of Aging*, **36**, 27–32.

[83] Biesbroek, J.M., Coenen, M., DeCarli, C., Fletcher, E.M., Maillard, P.M., Alzheimer's Disease Neuroimaging Initiative et al. (2024) Amyloid pathology and vascular risk are associated with distinct patterns of cerebral white matter hyperintensities: A multicenter study in 3132 memory clinic patients. *Alzheimer's & Dementia: The Journal of the Alzheimer's Association*, **20**, 2980–9.

[84] Lorenzini, L., Ansems, L.T., Lopes Alves, I., Ingala, S., Vállez García, D., Tomassen, J. et al. (2022) Regional associations of white matter hyperintensities and early cortical amyloid pathology. *Brain Communications*, **4**, fcac150.

[85] Pålhaugen, L., Sudre, C.H., Tecelao, S., Nakling, A., Almdahl, I.S., Kalheim, L.F. et al. (2021) Brain amyloid and vascular risk are related to distinct white matter hyperintensity patterns. *Journal of Cerebral Blood Flow and Metabolism: Official Journal of the International Society of Cerebral Blood Flow and Metabolism*, **41**, 1162–74.

[86] McCorkindale, A.N., Mundell, H.D., Guennewig, B. and Sutherland, G.T. (2022) Vascular Dysfunction Is Central to Alzheimer's Disease Pathogenesis in APOE e4 Carriers. *International Journal of Molecular Sciences*, **23**. https://doi.org/10.3390/ijms23137106

[87] Korte, N., Nortley, R. and Attwell, D. (2020) Cerebral blood flow decrease as an early pathological mechanism in Alzheimer's disease. *Acta Neuropathologica*, **140**, 793–810.

[88] Weijs, R.W.J., Shkredova, D.A., Brekelmans, A.C.M., Thijssen, D.H.J. and Claassen, J.A.H.R. (2023) Longitudinal changes in cerebral blood flow and their relation with cognitive decline in patients with dementia: Current knowledge and future directions. *Alzheimer's & Dementia: The Journal of the Alzheimer's Association*, Wiley. **19**, 532–48.

[89] Wang, Q., Schindler, S.E., Chen, G., Mckay, N.S., McCullough, A., Flores, S. et al. (2024) Investigating White Matter Neuroinflammation in Alzheimer Disease Using Diffusion-Based

Neuroinflammation Imaging. *Neurology*, **102**, e208013.

[90] Sachdev, P.S., Zhuang, L., Braidy, N. and Wen, W. (2013) Is Alzheimer's a disease of the white matter? *Current Opinion in Psychiatry*, **26**, 244–51.

[91] Nagaraja, N., DeKosky, S., Duara, R., Kong, L., Wang, W.-E., Vaillancourt, D. et al. (2023) Imaging features of small vessel disease in cerebral amyloid angiopathy among patients with Alzheimer's disease. *NeuroImage Clinical*, **38**, 103437.

[92] Reijmer, Y.D., van Veluw, S.J. and Greenberg, S.M. (2016) Ischemic brain injury in cerebral amyloid angiopathy. *Journal of Cerebral Blood Flow and Metabolism: Official Journal of the International Society of Cerebral Blood Flow and Metabolism*, **36**, 40–54.

[93] Vinters, H.V. and Gilbert, J.J. (1983) Cerebral amyloid angiopathy: incidence and complications in the aging brain. II. The distribution of amyloid vascular changes. *Stroke; a Journal of Cerebral Circulation*, **14**, 924–8.

[94] Szidonya, L. and Nickerson, J.P. (2023) Cerebral Amyloid Angiopathy. *Radiologic Clinics of North America*, **61**, 551–62.

[95] Roher, A.E., Tyas, S.L., Maarouf, C.L., Daugs, I.D., Kokjohn, T.A., Emmerling, M.R. et al. (2011) Intracranial atherosclerosis as a contributing factor to Alzheimer's disease dementia. *Alzheimer's & Dementia: The Journal of the Alzheimer's Association*, **7**, 436–44.

[96] Habes, M., Erus, G., Toledo, J.B., Bryan, N., Janowitz, D., Doshi, J. et al. (2018) Regional tract-specific white matter hyperintensities are associated with patterns to aging-related brain atrophy via vascular risk factors, but also independently. *Alzheimer's & Dementia: The Journal of the Alzheimer's Association*, **10**, 278–84.

[97] Paul, G. and Elabi, O.F. (2022) Microvascular Changes in Parkinson's Disease- Focus on the Neurovascular Unit. *Frontiers in Aging Neuroscience*, **14**, 853372.

[98] Fahn, S. and Sulzer, D. (2004) Neurodegeneration and neuroprotection in Parkinson disease. *NeuroRx: The Journal of the American Society for Experimental NeuroTherapeutics*, **1**, 139–54.

[99] Sonne, J., Reddy, V. and Beato, M.R. (2022) Neuroanatomy, Substantia Nigra. StatPearls Publishing.

[100] Hanyu, H., Imon, Y., Sakurai, H., Iwamoto, T., Takasaki, M., Shindo, H. et al. (1999) Regional differences in diffusion abnormality in cerebral white matter lesions in patients with vascular dementia of the Binswanger type and Alzheimer's disease. *European Journal of Neurology: The Official Journal of the European Federation of Neurological Societies*, **6**, 195–203.

[101] Hase, Y., Horsburgh, K., Ihara, M. and Kalaria, R.N. (2018) White matter degeneration in vascular and other ageing-related dementias. *Journal of Neurochemistry*, Wiley. **144**, 617–33.

[102] Khan, I. and De Jesus, O. (2023) Frontotemporal Lobe Dementia. StatPearls Publishing.

[103] Snowden, J.S., Adams, J., Harris, J., Thompson, J.C., Rollinson, S., Richardson, A. et al. (2015) Distinct clinical and pathological phenotypes in frontotemporal dementia associated with MAPT, PGRN and C9orf72 mutations. *Amyotrophic Lateral Sclerosis & Frontotemporal Degeneration*, **16**, 497–505.

[104] What are frontotemporal disorders? Causes, symptoms, and treatment [Internet]. National Institute on Aging.

[105] McMurtray, A.M., Chen, A.K., Shapira, J.S., Chow, T.W., Mishkin, F., Miller, B.L. et al. (2006) Variations in regional SPECT hypoperfusion and clinical features in frontotemporal dementia. *Neurology*, **66**, 517–22.

[106] Lindsay, K.W., Bone, I. and Fuller, G. (2010) Localised neurological disease and its management a. Intracranial. *Neurology and Neurosurgery Illustrated*, Elsevier. p. 217–388.

[107] Aswathy, P.M., Jairani, P.S., Raghavan, S.K., Verghese, J., Gopala, S., Srinivas, P. et al. (2016) Progranulin mutation analysis: Identification of one novel mutation in exon 12 associated with frontotemporal dementia. *Neurobiology of Aging*, **39**, 218.e1–3.

[108] Currens, L., Harrison, N., Schmidt, M., Amjad, H., Mu, W., Scholz, S.W. et al. (2023) A case of familial frontotemporal dementia caused by a progranulin gene mutation. *Clinical Parkinsonism & Related Disorders*, **9**, 100213.

[109] Sudre, C.H., Bocchetta, M., Heller, C., Convery, R., Neason, M., Moore, K.M. et al. (2019) White matter hyperintensities in progranulin-associated frontotemporal dementia: A longitudinal GENFI study. *NeuroImage Clinical*, **24**, 102077.

[110] Woollacott, I.O.C., Bocchetta, M., Sudre, C.H., Ridha, B.H., Strand, C., Courtney, R. et al. (2018) Pathological correlates of white matter hyperintensities in a case of progranulin mutation associated frontotemporal dementia. *Neurocase*, **24**, 166–74.

[111] Kazama, K., Hoshino, K., Kodama, T., Okada, M. and Yamawaki, H. (2017) Adipocytokine, progranulin, augments acetylcholine-induced nitric oxide-mediated relaxation through the increases of cGMP production in rat isolated mesenteric artery. *Acta Physiologica* , **219**, 781–9.

[112] Bruder-Nascimento, A., Awata, W.M.C., Alves, J.V., Singh, S., Costa, R.M. and Bruder-Nascimento, T. (2023) Progranulin Maintains Blood Pressure and Vascular Tone Dependent on EphrinA2 and Sortilin1 Receptors and Endothelial Nitric Oxide Synthase Activation. *Journal of the American Heart Association*, **12**, e030353.

[113] Jackman, K., Kahles, T., Lane, D., Garcia-Bonilla, L., Abe, T., Capone, C. et al. (2013) Progranulin deficiency promotes post-ischemic blood-brain barrier disruption. *The Journal of Neuroscience: The Official Journal of the Society for Neuroscience*, Society for Neuroscience. **33**, 19579–89.

[114] Martin, J.A., Craft, D.K., Su, J.H., Kim, R.C. and Cotman, C.W. (2001) Astrocytes degenerate in frontotemporal dementia: possible relation to hypoperfusion. *Neurobiology of Aging*, **22**, 195–207.

[115] Liu, C., Xie, S., Li, Y., Zhang, D., Li, D. and Zhang, C. (2024) Asymmetry in circulation system and cardiovascular diseases. *Medicine in Novel Technology and Devices*, **21**, 100283.

[116] Ni, L., Zhou, F., Qing, Z., Zhang, X., Li, M., Zhu, B. et al. (2020) The Asymmetry of White Matter Hyperintensity Burden Between Hemispheres Is Associated With Intracranial Atherosclerotic Plaque Enhancement Grade. *Frontiers in Aging Neuroscience*, **12**, 163.

[117] Ryu, W.-S., Schellingerhout, D., Ahn, H.-S., Park, S.-H., Hong, K.-S., Jeong, S.-W. et al. (2018) Hemispheric Asymmetry of White Matter Hyperintensity in Association With Lacunar Infarction. *Journal of the American Heart Association*, **7**, e010653.

[118] van Vuuren, A.J., Saling, M., Rogerson, S., Anderson, P., Cheong, J. and Solms, M. (2022) Cerebral Arterial Asymmetries in the Neonate: Insight into the Pathogenesis of Stroke. *Symmetry*, Multidisciplinary Digital Publishing Institute. **14**, 456.

[119] Ecury-Goossen, G.M., Raets, M.M.A., Camfferman, F.A., Vos, R.H.J., van Rosmalen, J., Reiss, I.K.M. et al. (2016) Resistive indices of cerebral arteries in very preterm infants: values throughout stay in the neonatal intensive care unit and impact of patent ductus arteriosus. *Pediatric Radiology*, **46**, 1291–300.

[120] Saba, L., Lucatelli, P., Anzidei, M., di Martino, M., Suri, J.S. and Montisci, R. (2018) Volumetric Distribution of the White Matter Hyper-Intensities in Subject with Mild to Severe Carotid Artery Stenosis: Does the Side Play a Role? *Journal of Stroke and Cerebrovascular Diseases: The Official Journal of National Stroke Association*, **27**, 2059–66.

[121] Lubben, N., Ensink, E., Coetzee, G.A. and Labrie, V. (2021) The enigma and implications of brain hemispheric asymmetry in neurodegenerative diseases. *Brain Communications*, **3**, fcab211.

[122] Burton, E.J., McKeith, I.G., Burn, D.J., Firbank, M.J. and O'Brien, J.T. (2006) Progression of white matter hyperintensities in Alzheimer disease, dementia with lewy bodies, and Parkinson disease dementia: a comparison with normal aging. *The American Journal of Geriatric Psychiatry: Official Journal of the American Association for Geriatric Psychiatry*, Am J Geriatr Psychiatry. **14**, 842–9.

[123] Holland, C.M., Smith, E.E., Csapo, I., Gurol, M.E., Brylka, D.A., Killiany, R.J. et al. (2008) Spatial distribution of white-matter hyperintensities in Alzheimer disease, cerebral amyloid angiopathy, and healthy aging. *Stroke; a Journal of Cerebral Circulation*, **39**, 1127–33.

[124] Meguro, K., Ishii, H., Kasuya, M., Akanuma, K., Meguro, M., Kasai, M. et al. (2007) Incidence of dementia and associated risk factors in Japan: The Osaki-Tajiri Project. *Journal of the Neurological Sciences*, **260**, 175–82.

[125] Bombois, S., Debette, S., Bruandet, A., Delbeuck, X., Delmaire, C., Leys, D. et al. (2008) Vascular subcortical hyperintensities predict conversion to vascular and mixed dementia in MCI patients. *Stroke; a Journal of Cerebral Circulation*, **39**, 2046–51.

[126] Sargurupremraj, M., Soumare, A., Bis, J.C., Surakka, I., Jurgenson, T., Joly, P. et al. (2023) Complexities of cerebral small vessel disease, blood pressure, and dementia relationship: new insights from genetics. *medRxiv : The Preprint Server for Health Sciences*,. https://doi.org/10.1101/2023.08.08.23293761

[127] Paternicò, D., Premi, E., Gazzina, S., Cosseddu, M., Alberici, A., Archetti, S. et al. (2016) White matter hyperintensities characterize monogenic frontotemporal dementia with granulin mutations. *Neurobiology of Aging*, **38**, 176–80.

[128] Sudre, C.H., Bocchetta, M., Cash, D., Thomas, D.L., Woollacott, I., Dick, K.M. et al. (2017) White matter hyperintensities are seen only in GRN mutation carriers in the GENFI cohort. *NeuroImage Clinical*, **15**, 171–80.

[129] Kang, S.W., Jeon, S., Lee, Y.-G., Park, M., Baik, K., Jung, J.H. et al. (2021) Implication of metabolic and dopamine transporter PET in dementia with Lewy bodies. *Scientific Reports*, **11**, 14394.

[130] Marshall, G.A., Shchelchkov, E., Kaufer, D.I., Ivanco, L.S. and Bohnen, N.I. (2006) White matter hyperintensities and cortical acetylcholinesterase activity in parkinsonian dementia. *Acta Neurologica Scandinavica*, **113**, 87–91.

[131] Wu, H., Hong, H., Wu, C., Qin, J., Zhou, C., Tan, S. et al. (2023) Regional white matter hyperintensity volume in Parkinson's disease and associations with the motor signs. *Annals of Clinical and Translational Neurology*, Wiley. **10**, 1502–12.

[132] Grimmer, T., Faust, M., Auer, F., Alexopoulos, P., Förstl, H., Henriksen, G. et al. (2012) White matter hyperintensities predict amyloid increase in Alzheimer's disease. *Neurobiology of Aging*, **33**, 2766–73.

[133] Kisler, K., Nelson, A.R., Montagne, A. and Zlokovic, B.V. (2017) Cerebral blood flow regulation and neurovascular dysfunction in Alzheimer disease. *Nature Reviews Neuroscience*, **18**, 419–34.

[134] Schoemaker, D., Zanon Zotin, M.C., Chen, K., Igwe, K.C., Vila-Castelar, C., Martinez, J. et al. (2022) White matter hyperintensities are a prominent feature of autosomal dominant Alzheimer's disease that emerge prior to dementia. *Alzheimer's Research & Therapy*, **14**, 89.

[135] Iturria-Medina, Y., Sotero, R.C., Toussaint, P.J., Mateos-Pérez, J.M., Evans, A.C. and Alzheimer's Disease Neuroimaging Initiative. (2016) Early role of vascular dysregulation on late-onset Alzheimer's disease based on multifactorial data-driven analysis. *Nature Communications*, **7**, 11934.

[136] Badhwar, A., Lerch, J.P., Hamel, E. and Sled, J.G. (2013) Impaired structural correlates of memory in Alzheimer's disease mice. *NeuroImage Clinical*, **3**, 290–300.

[137] Dadar, M., Mahmoud, S., Zhernovaia, M., Camicioli, R., Maranzano, J., Duchesne, S. et al. (2022) White matter hyperintensity distribution differences in aging and neurodegenerative disease cohorts. *NeuroImage Clinical*, **36**, 103204.

[138] McKhann, G.M., Knopman, D.S., Chertkow, H., Hyman, B.T., Jack, C.R., Jr, Kawas, C.H. et al. (2011) The diagnosis of dementia due to Alzheimer's disease: recommendations from the National Institute on Aging-Alzheimer's Association workgroups on diagnostic guidelines for Alzheimer's disease. *Alzheimer's & Dementia: The Journal of the Alzheimer's Association*, **7**, 263–9.

[139] Albert, M.S., DeKosky, S.T., Dickson, D., Dubois, B., Feldman, H.H., Fox, N.C. et al. (2011) The diagnosis of mild cognitive impairment due to Alzheimer's disease: recommendations from the National Institute on Aging-Alzheimer's Association workgroups on diagnostic guidelines for Alzheimer's disease. *Alzheimer's & Dementia: The Journal of the Alzheimer's Association*, **7**, 270–9.

[140] Vemuri, P., Graff-Radford, J., Lesnick, T.G., Przybelski, S.A., Reid, R.I., Reddy, A.L. et al. (2021) White matter abnormalities are key components of cerebrovascular disease impacting cognitive decline. *Brain Communications*, **3**, fcab076.

[141] Rundek, T., Tolea, M., Ariko, T., Fagerli, E.A. and Camargo, C.J. (2022) Vascular Cognitive Impairment (VCI). *Neurotherapeutics: The Journal of the American Society for Experimental NeuroTherapeutics*, **19**, 68–88.

[142] Beheshti, I., Potvin, O., Dadar, M. and Duchesne, S. (2024) Cerebrovascular lesion loads and accelerated brain aging: insights into the cognitive spectrum. *Frontiers in Dementia*, **3**, 1380015.

[143] Bernal, J., Schreiber, S., Menze, I., Ostendorf, A., Pfister, M., Geisendörfer, J. et al. (2023) Arterial hypertension and β-amyloid accumulation have spatially overlapping effects on posterior white matter hyperintensity volume: a cross-sectional study. *Alzheimer's Research & Therapy*, **15**, 97.

[144] Desmarais, P., Gao, A.F., Lanctôt, K., Rogaeva, E., Ramirez, J., Herrmann, N. et al. (2021) White matter hyperintensities in autopsy-confirmed frontotemporal lobar degeneration and Alzheimer's disease. *Alzheimer's Research & Therapy*, **13**, 129.

[145] Musa, G., Slachevsky, A., Muñoz-Neira, C., Méndez-Orellana, C., Villagra, R., González-Billault, C. et al. (2020) Alzheimer's Disease or Behavioral Variant Frontotemporal Dementia? Review of Key Points Toward an Accurate Clinical and Neuropsychological Diagnosis. *Journal of Alzheimer's Disease: JAD*, **73**, 833–48.

[146] Gainer, G. (2017) Frontotemporal Degeneration, Dementia - What is FTD? [Internet]. AFTD. The Association for Frontotemporal Degeneration.

[147] Beber, B.C. and Chaves, M.L.F. (2013) Evaluation of patients with behavioral and cognitive complaints: misdiagnosis in frontotemporal dementia and Alzheimer's disease. *Dementia & Neuropsychologia*, **7**, 60–5.

[148] (2023) Frontotemporal dementia [Internet]. Mayo Clinic.

[149] Egger, K., Rau, A., Yang, S., Klöppel, S., Abdulkadir, A., Kellner, E. et al. (2020) Automated voxel- and region-based analysis of gray matter and cerebrospinal fluid space in primary dementia disorders. *Brain Research*, **1739**, 146800.

[150] Yu, Q., Mai, Y., Ruan, Y., Luo, Y., Zhao, L., Fang, W. et al. (2021) An MRI-based strategy for differentiation of frontotemporal dementia and Alzheimer's disease. *Alzheimer's Research & Therapy*, **13**, 23.

[151] Brown, J.A., Lee, A.J., Fernhoff, K., Pistone, T., Pasquini, L., Wise, A.B. et al. (2023) Functional network collapse in neurodegenerative disease. *bioRxiv : The Preprint Server for Biology*,. https://doi.org/10.1101/2023.12.01.569654

[152] Varrone, A., Pappatà, S., Caracò, C., Soricelli, A., Milan, G., Quarantelli, M. et al. (2002) Voxel-based comparison of rCBF SPET images in frontotemporal dementia and Alzheimer's disease highlights the involvement of different cortical networks. *European Journal of Nuclear Medicine and Molecular Imaging*, **29**, 1447–54.

[153] Verfaillie, S.C.J., Adriaanse, S.M., Binnewijzend, M.A.A., Benedictus, M.R., Ossenkoppele, R., Wattjes, M.P. et al. (2015) Cerebral perfusion and glucose metabolism in Alzheimer's disease and frontotemporal dementia: two sides of the same coin? *European Radiology*, **25**, 3050–9.

[154] Steketee, R.M.E., Bron, E.E., Meijboom, R., Houston, G.C., Klein, S., Mutsaerts, H.J.M.M. et al. (2016) Early-stage differentiation between presenile Alzheimer's disease and frontotemporal dementia using arterial spin labeling MRI. *European Radiology*, **26**, 244–53.

[155] Du, A.T., Jahng, G.H., Hayasaka, S., Kramer, J.H., Rosen, H.J., Gorno-Tempini, M.L. et al. (2006) Hypoperfusion in frontotemporal dementia and Alzheimer disease by arterial spin labeling MRI. *Neurology*, **67**, 1215–20.

[156] Kim, W.S., Kågedal, K. and Halliday, G.M. (2014) Alpha-synuclein biology in Lewy body diseases. *Alzheimer's Research & Therapy*, **6**, 73.

[157] Stefanis, L. (2012) α-Synuclein in Parkinson's disease. *Cold Spring Harbor Perspectives in Medicine*, **2**, a009399.

[158] Zhao, W., Cheng, B., Zhu, T., Cui, Y., Shen, Y., Fu, X. et al. (2023) Effects of white matter hyperintensity on cognitive function in PD patients: a meta-analysis. *Frontiers in Neurology*, **14**, 1203311.

[159] Liu, H., Deng, B., Xie, F., Yang, X., Xie, Z., Chen, Y. et al. (2021) The influence of white matter hyperintensity on cognitive impairment in Parkinson's disease. *Annals of Clinical and Translational Neurology*, **8**, 1917–34.

[160] Oppedal, K., Aarsland, D., Firbank, M.J., Sonnesyn, H., Tysnes, O.B., O'Brien, J.T. et al. (2012) White matter hyperintensities in mild lewy body dementia. *Dementia and Geriatric Cognitive Disorders Extra*, **2**, 481–95.

[161] Olivari, B.S., Baumgart, M., Taylor, C.A. and McGuire, L.C. (2021) Population measures of subjective cognitive decline: A means of advancing public health policy to address cognitive health. *Alzheimer's & Dementia: The Journal of the Alzheimer's Association*, **7**, e12142.

[162] Parfenov, V.A., Zakharov, V.V., Kabaeva, A.R. and Vakhnina, N.V. (2020) Subjective cognitive decline as a predictor of future cognitive decline: a systematic review. *Dementia & Neuropsychologia*, **14**, 248–57.

[163] Giacomucci, G., Mazzeo, S., Padiglioni, S., Bagnoli, S., Belloni, L., Ferrari, C. et al. (2022) Gender differences in cognitive reserve: implication for subjective cognitive decline in women. *Neurological Sciences: Official Journal of the Italian Neurological Society and of the Italian Society of Clinical Neurophysiology*, **43**, 2499–508.

[164] Engedal, K., Barca, M.L., Høgh, P., Bo Andersen, B., Winther Dombernowsky, N., Naik, M. et al. (2020) The Power of EEG to Predict Conversion from Mild Cognitive Impairment and Subjective Cognitive Decline to Dementia. *Dementia and Geriatric Cognitive Disorders*, **49**, 38–47.

[165] Gouw, A.A., Alsema, A.M., Tijms, B.M., Borta, A., Scheltens, P., Stam, C.J. et al. (2017) EEG spectral analysis as a putative early prognostic biomarker in nondemented, amyloid positive subjects. *Neurobiology of Aging*, **57**, 133–42.

[166] Aschwanden, D., Sutin, A.R., Ledermann, T., Luchetti, M., Stephan, Y., Sesker, A.A. et al. (2022) Subjective Cognitive Decline: Is a Resilient Personality Protective Against Progression to Objective Cognitive Impairment? Findings from Two Community-Based Cohort Studies. *Journal of Alzheimer's Disease: JAD*, **89**, 87–105.

[167] Mazzeo, S., Padiglioni, S., Bagnoli, S., Bracco, L., Nacmias, B., Sorbi, S. et al. (2019) The dual role of cognitive reserve in subjective cognitive decline and mild cognitive impairment: a 7-year follow-up study. *Journal of Neurology*, **266**, 487–97.

[168] Bessi, V., Mazzeo, S., Padiglioni, S., Piccini, C., Nacmias, B., Sorbi, S. et al. (2018) From Subjective Cognitive Decline to Alzheimer's Disease: The Predictive Role of Neuropsychological Assessment, Personality Traits, and Cognitive Reserve. A 7-Year Follow-Up Study. *Journal of Alzheimer's Disease: JAD*, **63**, 1523–35.

[169] Reisberg, B., Shulman, M.B., Torossian, C., Leng, L. and Zhu, W. (2010) Outcome over seven years of healthy adults with and without subjective cognitive impairment. *Alzheimer's & Dementia: The Journal of the Alzheimer's Association*, **6**, 11–24.

[170] Stockmann, J., Verberk, I.M.W., Timmesfeld, N., Denz, R., Budde, B., Lange-Leifhelm, J. et al. (2020) Amyloid-β misfolding as a plasma biomarker indicates risk for future clinical Alzheimer's disease in individuals with subjective cognitive decline. *Alzheimer's Research & Therapy*, **12**, 169.

[171] Åberg, A.C., Petersson, J.R., Giedraitis, V., McKee, K.J., Rosendahl, E., Halvorsen, K. et al. (2023) Prediction of conversion to dementia disorders based on timed up and go dual-task test verbal and motor outcomes: a five-year prospective memory-clinic-based study. *BMC Geriatrics*, **23**, 535.

[172] Stickel, A.M., Tarraf, W., Gonzalez, K.A., Paredes, A.M., Zeng, D., Cai, J. et al. (2024) Cardiovascular disease risk exacerbates brain aging among Hispanic/Latino adults in the

SOL-INCA-MRI Study. *Frontiers in Aging Neuroscience*, **16**, 1390200.

[173] Sachdev, P.S., Parslow, R., Wen, W., Anstey, K.J. and Easteal, S. (2009) Sex differences in the causes and consequences of white matter hyperintensities. *Neurobiology of Aging*, **30**, 946–56.

[174] Fatemi, F., Kantarci, K., Graff-Radford, J., Preboske, G.M., Weigand, S.D., Przybelski, S.A. et al. (2018) Sex differences in cerebrovascular pathologies on FLAIR in cognitively unimpaired elderly. *Neurology*, **90**, e466–73.

[175] Lohner, V., Pehlivan, G., Sanroma, G., Miloschewski, A., Schirmer, M.D., Stöcker, T. et al. (2022) Relation Between Sex, Menopause, and White Matter Hyperintensities: The Rhineland Study. *Neurology*, **99**, e935–43.

[176] Morrison, C., Dadar, M., Collins, D.L. and Alzheimer's Disease Neuroimaging Initiative. (2024) Sex differences in risk factors, burden, and outcomes of cerebrovascular disease in Alzheimer's disease populations. *Alzheimer's & Dementia: The Journal of the Alzheimer's Association*, **20**, 34–46.

[177] Ng, K.P., Shen, J.Y., Chiew, H.J., Ng, A.S.L., Kandiah, N., Rosa-Neto, P. et al. (2023) White Matter Hyperintensity as a Vascular Contribution to the AT(N) Framework. *The Journal of Prevention of Alzheimer's Disease*, **10**, 387–400.

[178] Adlard, P.A., Tran, B.A., Finkelstein, D.I., Desmond, P.M., Johnston, L.A., Bush, A.I. et al. (2014) A review of β-amyloid neuroimaging in Alzheimer's disease. *Frontiers in Neuroscience*, **8**, 327.